이학박사학위논문

저산소-허혈에서 FADD에 의한 Necrosis 조절에 관한 연구

A study on the FADD-mediated necrosis in response to hypoxia-ischemia

2015년 8월

서울대학교 대학원

유전공학 협동과정

최 선 국

ABSTRACT

A study on the FADD-mediated necrosis in response to hypoxia-ischemia

Seon-Guk Choi
Interdisciplinary
Graduate Program
in Genetic Engineering
Seoul National University

Fas-associated protein with death domain (FADD) plays a key role in recruiting and activating initiator caspases in the extrinsic apoptosis. However, increasing evidence indicate that FADD is also involved in intrinsic cell death, cell proliferation and necroptosis, indicating multiple functions of FADD in diverse signaling. Here I showed that FADD is dynamically modified by SUMO2 *in vitro* and *in vivo* at multiple lysine sites K120/125/149. This SUMOylation was mediated by E3 SUMO ligase PIAS3 and reversed by SENP6 and 7. Notably, FADD SUMOylation

occurred during necrosis following the treatment with high dose of calcium ionophore A23187 in HeLa cells. Calcium overload initiated FADD translocation on the mitochondria, which promoted Drp1 translocation on the mitochondria as well. Treatment with A23187 induced Drp1–mediated mitochondrial fragmentation in a FADD SUMOylation-dependent manner. The necrosis triggered by A23187 was blocked in Drp1- or FADD-deficient mouse embryonic fibroblasts and ectopic expression of SUMOylation-defective FADD 3KR mutant. I showed that Drp1 binds to SUMOylated FADD *in vitro* and in cells. FADD and Drp1 bound to Mff in the mitochondrial. In addition, FADD SUMOylation and its translocation on the mitochondria occurred in culture cells undergoing hypoxia-induced and calcium-dependent necrosis and in ischemic damaged core resulting from middle cerebral artery occlusion (MCAO) in the mouse brain**.** Strikingly, calcium overload-induced cell death was also blocked by knockdown of caspase-10 but not of caspase-8. However, A23187- and mitochondrial FADD-induced mitochondrial fragmentation drove caspase-independent necrotic death. Interestingly, caspase-10 formed a protein complex with FADD and Drp1 on the mitochondria and potentiates A23187-induced necrosis and Drp1 oligomerization. Furthermore, activity-dead caspase-10 V410I and L285F mutants, which are observed in autoimmune lymphoproliferative syndrome and inhibits TRAIL-induced apoptosis,

enhanced Drp1 oligomerization. Together this study reveals a novel role of SUMO modification of FADD in the calcium stress-induced, Drp1- and caspase-10-dependent mitochondrial fragmentation and regulated necrosis, providing insight into the mechanism of hypoxic and ischemia injury in a range of pathologies.

Key words: FADD (Fas-associated protein with a death domain), Drp1 (Dynamin-related protein 1), mitochondrial fragmentation, caspase-10, PIAS3 (protein inhibitor of activated STAT3), regulated necrosis, SUMOylation

Student Number : 2007-22808

TABLE OF CONTENTS

LIST OF FIGURES

ABBREVIATION

BAPTA	1,2-Bis(o-aminophenoxy)ethane-N,N,N',N'-tetraacetic acid
Caspase	Cysteine-aspartic protease
DD	Death domain
DED	Death effector domain
Drp1	Dynamin-related protein 1
DTT	Dithiothreitol
FADD	Fas-associated protein with a death domain
FAS	Fas cell surface death receptor
FBS	Fetal bovine serum
Fis1	Fission 1 (mitochondrial outer membrane) homolog (S. cerevisiae)
GFP	Green fluorescence protein
GST	Glutathione S-transferase
HA	Hemagglutinin
IP	Immunoprecipitation
IPTG	Isopropyl β-D-1-thiogalactopyranoside
MCAO	Middle cerebral artery occlusion
MEF	Mouse embryonic fibroblast
MiD49	Mitochondrial dynamics proteins of 49 kDa

Mff	Mitochondrial fission factor
MPTP	Mitochondrial permeability transition pore
PBS	Phosphate buffered saline
PCD	Programmed cell death
PFA	Paraformaldehyde
PI	Propidium iodide
PIAS3	Protein inhibitor of activated STAT3
SENP	Sumo-specific isopeptidase
SUMO	Small ubiquitin-like modifier
TNFα	Tumor necrosis factor alpha
TRAIL	TNF-related apoptosis-inducing ligand
UBC9	Ubiquitin carrier protein 9

Introduction

Programmed cell death (PCD) is classified into three morphological and biochemical types: apoptosis, autophagic cell death and necrosis. Fas-associated protein with a death domain (FADD) is an essential adaptor in TNF family-mediated extrinsic apoptosis. Upon death ligand-binding, interaction between death domains (DD) of membrane-bound death receptors (DR) and DD of FADD recruits caspase-8 or -10 through another homophilic interaction of death effector domains (DED) to form a death-inducing signaling complex (DISC). Initiator caspases are then activated and bursts subsequent activation of downstream caspases leading to apoptosis (Chinnaiyan et al. 1995; Kischkel et al. 1995; Zhang and Winoto 1996). Impairment in cell death regulation can be a component of various diseases such as cancer, autoimmune lymphoproliferative syndrome (ALPS) and neurodegenerative diseases, AIDS and ischemia (Reed 2002). On the other, FADD has a versatile role in cell proliferation and non-receptor-mediated apoptosis. Regulation of FADD phosphorylation status by casein kinase Iα or AK2-DUSP26 seems to be a key factor that determines the nuclear localization of FADD during cell cycle progression, resulting in tumor

development (Kim et al. 2014). In a recent study, germline disruption or ubiquitination of FADD enhances TNFα-induced programmed necrosis, called necroptosis (Welz et al. 2011; Zhang et al. 2011; Lee et al. 2012). This type of cell death is not blocked by caspase inhibitors and depends on RIP1, RIP3 and the mixed lineage kinase domain-like (MLKL), but the requirement of Drp1 is controversial (Moujalled et al. 2014). In addition, increasing studies also revealed that FADD gives rise to caspase-independent necrosis but the mechanism is not discovered yet (Kawahara et al. 1998; Matsumura et al. 2000).

Based on the sequence homology, caspase-10 and caspase-8 have been proposed to be component of DISC complex to initiate apoptosis. However, studies investigating this hypothesis reported some conflicting results for the roles of those caspases (Juo et al. 1998; Teitz et al. 2000). In addition to the proposed role in the extrinsic apoptosis, caspase-10 is responsible for drug-induced intrinsic apoptosis in several types of cancer cells by forming AK2-FADD-Caspase10 complex (Lee et al. 2007) and inhibits autophagy by cleaving BCLAF1, a strong inducer of autophagy (Lamy et al. 2013). Furthermore, overexpressed caspase-10 can activate the NF-κB pathway (Chaudhary et al. 2000). More interestingly, caspase-10 mutation is associated with ALPS type II but these caspase-10 mutations do

not affect TNF or CD95L-induced apoptosis (Wang et al. 1999). Other apoptosis-independent caspase-10 mutations were also discovered in several primary tumors or tumor cell lines from different origin (Harada et al. 2002; Park et al. 2002; Shin et al. 2002). However, these functions of caspase-10 and its mutants are not clear yet.

SUMOylation is a post-translational modification of substrate proteins via covalent attachment with small ubiquitin-like modifier (SUMO). Like ubiquitination, SUMO conjugation system utilizes a unique E1-activating enzyme complex formed by a heterodimer SAE1/SAE2 (Aos1/Uba2), an E2-conjugating enzyme Ubc9 and E3 ligases including PIASs, RanBP2 and polycomb protein Pc2. Reversibly SUMO proteins are deconjugated from the substrate by SUMO-specific isopeptidases (SENPs) (Melchior et al. 2003; Johnson 2004). Many SUMO acceptable lysines lie within a consensus ΨKX(E/D) motif (ψ, hydrophobic amino acid and X, any amino acid) (Hay 2005). However, recent proteomics studies reveal that numerous proportion of SUMOylated proteins do not include the consensus sites (Blomster et al. 2009; Golebiowski et al. 2009; Hsiao et al. 2009). Substrate modification by SUMO is known to govern diverse cellular functions, including transcription, intracellular transport, DNA repair, replication and cell cycle progression (Gill 2004). Moreover, SUMO conjugation can

change intracellular localization of substrate by transforming structure of substrate and subsequently alter protein-protein interaction. In addition, increasing evidences have shown that some proteins in cell death pathways, including p53, NEMO or caspases, are substrates for the SUMO conjugation system, allowing for the exploration of a novel involvement of SUMO in cell death signaling (Huang et al. 2003; Besnault-Mascard et al. 2005; Bischof et al. 2006).

Mitochondria are essential organelles that execute wide range of functions, from production of ATP through oxidative phosphorylation and buffering cytosolic or ER containing [Ca^{2+}] levels to differentiation and regulation of programmed cell death (McBride et al. 2006). Mitochondrial morphology changes dynamically by continuously undergoing fusion and fission in balance. The equilibrium is shifted toward highly interconnected networks or complete fragmentation to form small round vesicles in respond to various stimuli. Mitochondrial integrity and function are closely connected and aberration in this regulation may occur in neurodegenerative disease and metabolic disorder (Varadi et al. 2004; Gustafsson and Gottlieb 2008; Shirendeb et al. 2011; Sheng et al. 2012). Mitochondrial fusion and fission are regulated by a family of large GTPases. Mitofusin proteins (Mfn1 and Mfn2) of MAM and Optical atrophy 1 (Opa1) in inner

membrane are involved in fusion, whereas dynamin-related protein 1 (Drp1) controls mitochondrial fission (Chan 2006; Knott et al. 2008). During mitochondrial fission, Drp1 is translocated from the cytosol onto the mitochondrial outer membrane, where it oligomerizes and, through hydrolysis of GTP, changes its conformation to sever the mitochondrial tubule (Mears et al. 2011). Drp1-dependent fission is regulated by leading to bind to mitochondrial Drp1 receptors, such as Fis1, Mff, MiD49 and MiD51 and undergoing posttranslational modification or undergoing posttranslational modification, which regulates the activity (Otera et al. 2013). Drp1 is essential for synapse formation (Ishihara et al. 2009), but Drp1-mediated excessive mitochondrial fragmentation trigger apoptosis, autophagic cell death and necrosis in response to various stimuli (Iglewski et al. 2010; Whelan et al. 2012; Liu et al. 2013). Notably, alteration of mitochondrial dynamics is closely related to hypoxia/ischemia induced cell death (Kim et al. 2011). However, the mechanism through which Drp1 is recruited to the mitochondria and induce necrosis during ischemia is more elucidative.

Here, I identify that SUMO2 is conjugated to three non-consensus lysine residues of FADD in response to excessive calcium overload. SUMOylated FADD is forced to translocate onto mitochondria and induce mitochondrial

fragmentation. I further demonstrate that SUMOylated FADD is essential for the recruitment of cytosolic Drp1 to the mitochondria and trigger caspase-independent necrosis during hypoxic and ischemic injury.

Results

FADD is modified by SUMO-1 and 2.

In an effort to elucidate whether FADD is a target of SUMOylation, I performed *in silco* modeling analysis. SUMO sp2.0 predicted that FADD has one non-consensus motif at Lys 125 (TKID) [37]. To test this prediction, I first examined whether FADD could be modified by SUMO in cells. HEK293T cells were co-transfected with vectors encoding HA-tagged human FADD along with Flag-tagged E2 ligase Ubc9 and His_6-tagged SUMO isoform 1 or 2 in the presence of IDN-5665, an inhibitor of caspases because the overexpression of FADD initiated apoptotic cell death. His-tagged SUMO conjugated proteins were isolated using Ni-NTA agarose beads under 5% SDS denaturing condition and added N-ethylmaleimide to inhibit the action of SUMO proteases. From immunoblotting of the beads bound proteins, I found larger FADD protein (~ 50 kDa) strongly SUMOylated with SUMO2 than HA-tagged FADD (~ 30 kDa) (Fig. 1A, upper). I also could detect the SUMOylated FADD in cell lysates with immunoblot analysis (Fig. 1A, lower)

In next step, I analyzed whether FADD could be conjugated to SUMO2 *in vitro*. Recombinant GB1-tagged FADD protein was purified

form *E. coli* and then incubated with purified GST-tagged SAE1/2 (E1), His-tagged Ubc9 (E2) and GST-tagged SUMO2 in the absence or presence of DTT. After incubation for the increasing periods, samples were subjected to immunoblot assay using anti-FADD antibody. Consistent to that in cells, incubation with SUMO2 resulted in robust GST-fused SUMO2 conjugation of FADD as indicated by the high molecular weight (~ 80 kDa) (Fig. 1B). Similar results were observed in *E.coli* SUMOylating system. His-FADD and E1, E2, SUMOs were co-expressed by IPTG treatment in *E.coli* [38]. Immunoblotting with anti-FADD antibody revealed a shifted band in bacteria lysates expressing His-FADD and either pT-E1E2SUMO1 or 2, but not in the lysates expressing FADD only (Fig. 1C).

To further investigate which E3 SUMO ligases regulated FADD SUMOylation, each of PIAS1, xα, 3, and γ was co-transfected with FADD and SUMO2 into HEK293T cells. Among them, overexpression of PIAS3 markedly increased SUMOylation of FADD (Fig. 2D). To identify FADD-specific deSUMOylating enzyme, each of SENP1 (Fig. 2B), SENP2 (Fig. 2C) and SENP5-7 (Fig.2D) was overexpressed with SUMO2. Among the human SENPs, only SENP6 and 7 reduced FADD SUMOylation markedly.

Calcium-overload causes FADD SUMOylation in death domain

To identify the signals which induce FADD SUMOylation, I exposed HeLa cells to various insults, including TNF-α and cycloheximide or FAS ligand to trigger extrinsic apoptosis and etoposide or thapsigargin to initiate intrinsic apoptosis [39]. In these conditions, I could not detect SUMOylated FADD (Fig. 3A). In recent studies, FADD served as a negative regulator of RIP1-RIP3 complex which mediates necroptosis. When I thus examined FADD SUMOylation under necrotic conditions, I treated the combination of TNF-α, smac mimetic and caspase inhibitor IDN-5665 to trigger necroptosis or high dose of A23187 to induce intrinsic necrosis in HeLa cells expressing RIP3 [40]. Strikingly, I found that FADD was conjugated with SUMO2 under high dose of A23187 in HeLa cells and not during treatment with T/S/I (Fig. 3B). I could observe SUMOylated FADD in HeLa cells exposed to high doses more than 5 μM of A23187 but not in low doses less than 0.5 and 2 μM of it (Fig. 4A). In addition, FADD SUMOylation at high dose of A23187 increased until 6 h and then declined thereafter (Fig. 4B). From the immunoprecipitation and immunoblot assays, I apparently found SUMOylated FADD in A23187-treated HeLa cells (Fig. 4C). Moreover, the FADD-PIAS3 interaction was increased by A23187 treatment (Fig. 5). These results suggest that FADD is SUMOylated under calcium overload-induced cell death.

In order to find out the SUMO acceptable lysines in FADD, I performed mutagenesis which introduced arginine by replacing all 8 lysine sites. Pull-down assays following ectopic expression of FADD mutants, Ubc9 and SUMO2 in HEK293T cell revealed that mutation at lysine 125 (K125R) or 149 (K149R) in the death domain (DD) of FADD partially reduced the intensity of SUMO-conjugated FADD (Fig. 6A). Thus, I generated double FADD mutant containing arginine at both lysine 125 and 149 (K125/149R) and combinations of proximate lysine 120 (K120/125R, K120/149R). However, these FADD 2KR double mutations could not still completely abolish FADD SUMOylation (Fig. 6B).

Accordingly, in addition to FADD 2KR, I introduced one more lysine-to-arginine mutation at lysine 120 into FADD 2KR double mutant (K125/149R). The same assays revealed that FADD 3KR (K120/125/149R) triple mutation strongly impaired FADD SUMOylation (Fig. 7A). To test whether these 3 lysines (120, 125, 149) are required for conjugation with SUMO2 in cells under high dose of A23187 treatment, I treated HeLa cells with A23187 after ectopic expression of FADD wild-type or 3KR mutant. I contrast to the SUMOylation of FADD wild-type, FADD 3KR mutant was not SUMOylated (Fig, 7B). Together these results indicate that FADD is modified by SUMO2 at lysine 120, 125 and 149 under excessive calcium

overload.

SUMOylated FADD is translocated to mitochondria for mitochondria fragmentation

In the previous study, severe calcium stress provokes translocation of the gamut of proapoptotic and necrogenic cytoplasm-residual factors (Bax, p53, PGAM5, Drp1) to the mitochondria [40-43]. Interestingly, I found that the treatment of HeLa cells with A23187 increased FADD in the mitochondria rich-fraction, while it reduced FADD in the cytosol rich-fraction (Fig. 8A). As reported, Drp1 and p53 were accumulated in the mitochondrial fraction upon calcium overload. Immunocytochemical analysis also revealed that FADD very much colocalized with the immunoreactivity against TOM20, a mitochondrial outer membrane protein, while FADD was in the cytosol with diffused pattern in untreated control cells (Fig. 8B). Especially, SUMOylated FADD was detected in the both cytosolic and mitochondrial fractions at 3 h after A23187 treatment (Fig. 8C). These results indicate that calcium stress causes FADD translocation to the mitochondria.

Excessive cytosolic calcium overloading or accumulation of oxidative stress brings about opening of the mitochondrial permeability

transition pore (MPTP) and subsequent mitochondrial permeability transition (mPT) for the dissipation of the mitochondrial membrane potential ΔΨm [44]. To examine whether FADD is required for A23187-induced mPT, I performed Calcelin/Cobalt-bleaching assay. Treatment with A23187 in FADD wild-type and knockout MEFs did not affect rapidly MPTP formation until 3 h (Fig. 9A and 9B). Interestingly, at 3 hour time point mitochondrial morphology was changed to dot- or sphere-like shape in FADD wild-type MEFs and not in KO MEFs (Fig. 9A). As reported [42], I observed fragmented mitochondria under calcium-overload condition. Due to this similarity, I investigated whether A23187-mediated mitochondrial fragmentation was regulated by FADD.

The treatment of FADD wild-type MEFs after ectopic expressing of mito-YFP with A23187 triggered dramatic mitochondrial fragmentation in early time points. Interestingly A23187-induced mitochondria fission and aggregate formation were significantly inhibited in FADD knock-out MEFs (Fig. 10A), the numbers of cells with fragmented mitochondria were reduced from 60 % to 20 % by FADD deficiency (Fig. 10B). Further, I examined whether the mitochondrial fragmentation requires FADD SUMOylation using FADD-3KR mutant. I found that HeLa cells ectopic expressing of FADD-WT underwent about 20 % more rapid fragmentation

than HeLa cells and 3KR over-expressing HeLa cells (Fig. 11). These results indicate that SUMOylated FADD is accumulated on mitochondria and it is required for mitochondrial fragmentation under calcium overload.

SUMOylated FADD interacts with Drp1 to affect Drp1 translocation onto mitochondria

Since I observed that Drp1, a crucial regulator of mitochondria fission [45], was accumulated in the mitochondria upon A23187 treatment and FADD was required for mitochondrial fragmentation (Fig. 8A and 10B), I hypothesized that FADD-mediated mitochondrial fragmentation was dependent on Drp1 activity. To test this hypothesis, I examined the effect of Drp1 K38A dominant negative mutant on the mitochondrial fragmentation. Interestingly, ectopic expression of Drp1 dominant negative mutant abolished FADD-induced mitochondrial fragmentation (Fig. 12), indicating that Drp1 is required for FADD-induced mitochondrial fragmentation. I further addressed an important question how FADD functionally regulates Drp1 activity. More interestingly, from the immunoprecipitation assay, I found that FADD interacted with Drp1 in the cytosol fraction and similarly in the mitochondria fraction under calcium stress (Fig. 13).

Covalently conjugated SUMO residue is usually utilized as a new

docking site to interact with target proteins which have SUMO interacting motif (SIM) [46] or by masking the protein-interacting surfaces [19]. To elucidate whether FADD SUMOylation was essential for the interaction of FADD with Drp1, I performed the immunoprecipitation assay using HA-FADD WT or 3KR mutant. The results illustrated that FADD WT did not interact with Drp1 in untreated control cells. However, the treatment with A23187 induced the interaction of FADD with Drp1 in the cytosol and mitochondria fractions. In contrast to FADD WT, FADD 3KR mutant failed to interact with Drp1 in the absence or presence of A23187 (Fig. 14A). In addition, SUMOylated FADD showed much higher affinity to Drp1 protein than unmodified FADD (Fig. 14B). Further, when I addressed which mitochondrial Drp1 receptor/adaptor was utilized for FADD/Drp1-mediated mitochondrial fragmentation, I found that Mff bound to FADD under calcium stress but other receptors Fis1, MiD49 and MiD51 did not (Fig. 15A). In the same protein complex, I also detected Drp1. These results suggest that calcium stress induces the formation of FADD-Drp1-Mff complex to accept cytosolic FADD-Drp1 onto the mitochondria.

In addition, lack of FADD expression ameliorated the recruitment of Drp1 to the mitochondrial fraction (Fig. 15B). These results indicated that

FADD SUMOylation is required for its interaction with Drp1 and the recruitment of Drp1 to the mitochondria in response to calcium overload.

FADD SUMOylation is required for caspase-independent and hypoxic cell death

Two types of cell death, apoptosis and necrosis, can occur by calcium overload depending on its duration or concentration [47, 48]. In general, excessive calcium influx or overload induces Drp1-dependent mitochondria fission, which mediates not only apoptosis [49] but necrotic cell death [40]. To address what types of cell death is evoked by high dose of calcium, I determined cell death mode. Cell death induced by low dose (2 μM) of A23187 was completely suppressed by IDN-5665, a pan caspase inhibitor. In contrast, cell death by high dose (5 μM) of A23187 was not inhibited but rather potentiated by IDN-5665, as judged by the staining with propidium iodide (PI), which permeates into the disrupted plasma membrane of necrotic cells (Fig. 16A). Consistently, caspase-8 and 9 were cleaved for their activation by TNFα and cycloheximide or lose dose (2 μM) of A23187, but not by high dose, in HeLa cells (Fig. 16B). I also confirmed the release of cytochrome c into the cytosol fraction by high dose (20 μM M) of A23187 (Fig. 16C) did not occur and early rupture of plasma

membrane by it (data not shown). These observations indicate that high dose (> 5 μM) of A23187 induces caspase-independent necrosis.

When I addressed whether FADD or Drp1 was required for A23187-induced necrosis, I found that FADD knockout MEFs inhibited PI-positive cell death induced by high dose of A23187 (Fig. 17A). Similarly, deficiency of Drp1 expression also interfered with A23187-induced cell death. Further, I investigated the necessity of SUMO modification of FADD during A23187-induced necrosis. Ectopic expression of FADD WT potentiated the A23187-induced necrosis, on the contrary, FADD 3KR mutant showed less effect than FADD WT on A23187-induced necrosis (Fig. 17B). In sum, these results demonstrate that SUMO modified-FADD is required for caspase-independent necrotic cell death which is caused by high dose of A23187.

Both excessive calcium influx and intracellular accumulation for calcium overload are frequently observed under ischemia and hypoxia [50]. To examine FADD SUMOylation and its role in the physiological model of hypoxia, I first examined whether FADD is SUMOylated due to intense calcium influx under low oxygen availability in HeLa cells. HeLa cells were incubated in normoxic (O_2 20%) or hypoxic (O_2 1%) condition for 24 h in the presence of BAPTA-AM, an intracellular Ca^{2+} chelator. Immunoblot

analysis revealed that FADD was SUMOylated at 24 h in hypoxia but chelation of intracellular Ca^{2+} prevented the hypoxia-induced SUMOylation of FADD in HeLa cells (Fig. 18A). Next, I tested whether hypoxia and reoxygenation leads to increased FADD SUMOylation. When HeLa cells were exposed to hypoxic condition for 24 h and subsequent reoxygenation for 2 and 4 h, the level of SUMOylated FADD was detected at 2 h and then decreased thereafter (Fig. 18B).

As expected, the translocation of FADD to mitochondria also occurred at 24 h during hypoxia and most prominent at 48 h (Fig. 18C). In addition, knock-down of FADD expression reduced the hypoxia-induced cell death (Fig. 19). Interestingly, HeLa cells, which defected FADD expression, were decreased cell death by treatment with caspase inhibitor. It is indicated that hypoxia trigger apoptosis as well as necrosis and FADD is a key regulator of necrosis. Moreover, when I examined SUMOylation of FADD in the mouse brains after ischemic injury, I found that mouse FADD was SUMOylated in ischemic damage core resulting from middle cerebral artery occlusion (MCAO) in mice (Fig. 20A). Beside, ischemic damages increased the interaction of mouse FADD and Drp1 (Fig. 20B). As expected, FADD was found in the cytosol in control brain but was enriched in the mitochondrial fraction following ischemic damage (Fig. 20C). These results

indicate that FADD is SUMOylated and translocate into the mitochondria during hypoxic/ischemic injury.

Caspase-10 is recruited to the mitochondria for Drp1 oligomerization

FADD SUMOylation following intracellular calcium overload induces cell death which was not prevented by caspase inhibitor IDN-5665 (Fig. 16A). To confirm caspase-independent cell death of calcium overload-induced mitochondrial fragmentation, I reduced the expression of caspase-8 or -10 by utilizing caspase-specific shRNA in HeLa cells. Interestingly, knockdown of caspase-10 expression blocked A23187-induced mitochondrial fragmentation (Fig. 21A). In contrast, knockdown of caspase-8 expression did not affect the mitochondrial fragmentation. I further evaluated the function of caspase-10 in the mitochondrial fragmentation. Ectopic expression of caspase-10 did not influence the translocalization of Drp1 and FADD onto the mitochondria in MCF7 cells, which rarely express caspase-10 [6]. On the contrary, upon treatment with high dose of A23187. caspase-10 greatly influenced Drp1 and FADD accumulation on the mitochondria (data not shown). Next, I examined whether caspase-10 also is recruited into FADD-Drp1 complex under high dose of A23187 in FADD wild-type MEFs. Due to lack of caspase-10 in MEFs, FADD wild-type or

knock-out MEFs were transfected with human caspase-10 and then treated with high dose of A23187. Treatment with A23187 recruited FADD and caspase-10 into Drp1, forming a protein complex in FADD wild-type MEFs, but not in FADD knock-out MEFs (Fig. 22A), indicating that FADD serves as an adaptor for the interaction of caspase-10 with Drp1. Further, to examine the subcellular localization of caspase-10 for its interaction with Drp1, HeLa cells were subjected to subcellular fractionation and the fractions were analyzed by immunoprecipitation assays using anti-FADD antibody. Interestingly, I found the interaction of FADD with caspase-10 only in the mitochondria-rich fraction, but not in the cytosolic fraction, following A23187 treatment (Fig. 22B). In contrast, caspase-8 was not detected in the protein complex in the mitochondrial fraction. Moreover, a marked increase of Drp1 oligomerization was observed in HeLa cells showing the formation of caspase-10 and FADD complex (Fig. 22B).

In ALPs type II, mutation of *Caspase-10* at L285F or V410I was reported to impair apoptosis and expression of this mutant abrogates caspase-10-mediated apoptosis through its dominant-negative interaction with wild-type caspase-10 in HeLa and MCF7 cells [51]. Thus, I addressed whether these mutations affect FADD- and Drp1-mediated cell death. Consistent to the previous reports, overexpression of caspase-10 L285F or

V410I mutant prevented TRAIL-induced cell death in MCF7 cells (Fig. 23A). Surprisingly, A23187-induced cell death and mitochondrial fragmentation were accelerated by ectopic expression of not only caspase-10 wild-type but also L285F and V410I mutants (Fig. 23B and C). Furthermore, Drp1 oligomerization occurs together with the formation of FADD-Drp1-Caspase10 protein complex (Fig. 23C). In addition, I found that caspase-10 wild-type, V410I mutant and death effector domain (DED) of caspase-10 were all required for Drp1 oligomerization in MCF7 cells during calcium overload (Fig. 24). These results indicate that caspase-10 enhances Drp1 oligomerization regardless of its apoptosis-inducing activity under calcium overload.

Figure 1. Modification of FADD by SUMO isoforms.

(A) HEK293T cells were transfected with HA-FADD alone or together with Flag-Ubc9 and His-SUMO-1 or 2 in the presence of 25 μM IDN. After 24 h, cell extracts were subjected to pull-down assay using Ni^{2+}-NTA agarose beads under denaturing condition (5% SDS) and the bound proteins were analyzed by immunoblot assay (IB) using the indicated antibodies (upper). Whole cell lysates (Input, 1/10 of IP) were immunoblotted with anti-HA, Xpress and Flag antibodies as a control (lower).

(B) Purified GB1-FADD protein was incubated with purified GST-Aos1/Uba2, His-Ubc9, and GST-SUMO2 (-GG) proteins in the absence or presence of DTT (100 μM) at 37℃ for the indicated times and then subjected to immunoblot analysis using anti-FADD antibody.

(C) *E.coli* BL21 cells were transformed with pET-FADD alone or in combination with pET-E1E2SUMO1 or pET-E1E2SUMO2 which encodes SUMO enzyme E1, E2 and SUMO1 or 2 (-GG). After being treated with IPTG (1 mM) at 37℃ for 6 h, cells were analyzed by immunoblotting using anti-FADD antibody.

Figure 1

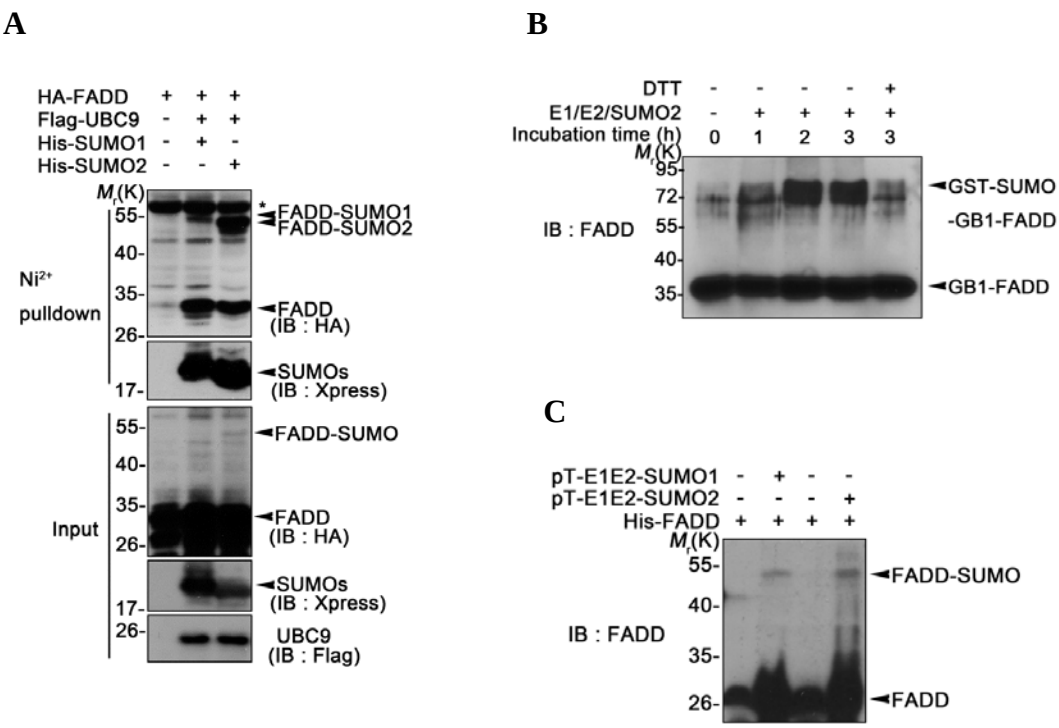
A
HA-FADD + + +
Flag-UBC9 - + +
His-SUMO1 - + -
His-SUMO2 - - +
M_r(K)
55-
40-
35-
26-
17-
Ni2+
pulldown
*
FADD-SUMO1
FADD-SUMO2
FADD
(IB : HA)
SUMOs
(IB : Xpress)
55-
40-
35-
26-
17-
26-
Input
FADD-SUMO
FADD
(IB : HA)
SUMOs
(IB : Xpress)
UBC9
(IB : Flag)
B
DTT - - - - +
E1/E2/SUMO2 - + + + +
Incubation time (h) 0 1 2 3 3
M_r(K)
95-
72-
55-
40-
35-
IB : FADD
GST-SUMO
-GB1-FADD
GB1-FADD
C
pT-E1E2-SUMO1 - + - -
pT-E1E2-SUMO2 - - - +
His-FADD + + + +
M_r(K)
55-
40-
35-
26-
IB : FADD
FADD-SUMO
FADD

Figure 2. PIAS3, SENP6 and SENP7 regulate FADD SUMOylation in the transfected cells.

(A) HEK293T cells were cotransfected with HA-FADD, His-SUMO2 and Flag-PIAS-1, xα, 3 or γ in the presence of 25 μM IDN for 24 h and cell extracts were pulled-down with Ni^{2+}- NTA agarose beads under denaturing condition (5% SDS) and the bound proteins were analyzed by immunoblot assay (IB) using the indicated antibodies (upper). Whole cell lysates (Input, 1/10 of IP) were immunoblotted with indicated antibodies as a control (lower).

(B-D) HEK293T cells were transfected with His-SUMO2 and Myc-SENP1 (B), Flag-SENP2 (C) or Flag-SENP- 5,6,7 (D) in the presence of 25 μM IDN for 24 h and cell extracts were pulled-down with Ni^{2+}- NTA agarose beads as described in (A).

Figure 2

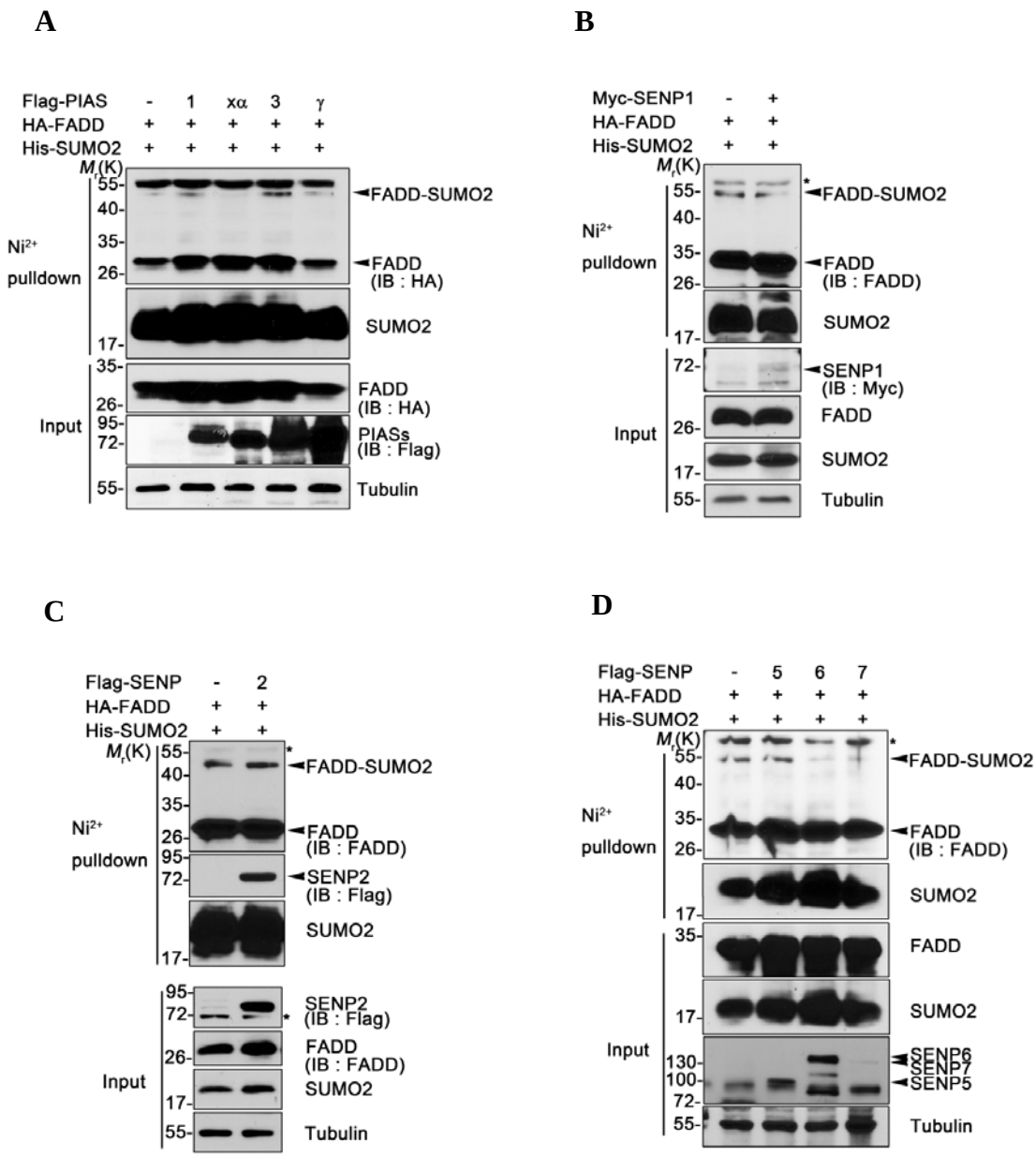
A
Flag-PIAS - 1 xα 3 γ
HA-FADD + + + + +
His-SUMO2 + + + + +
Mr(K)
55-
40-
35-
26-
17-
Ni2+ pulldown
FADD-SUMO2
FADD (IB : HA)
SUMO2
Input
35-
26-
95-
72-
55-
FADD (IB : HA)
PIASs (IB : Flag)
Tubulin
B
Myc-SENP1 - +
HA-FADD + +
His-SUMO2 + +
Mr(K)
55-
40-
35-
26-
17-
72-
Ni2+ pulldown
Input
FADD-SUMO2
FADD (IB : FADD)
SUMO2
SENP1 (IB : Myc)
FADD
SUMO2
Tubulin
C
Flag-SENP - 2
HA-FADD + +
His-SUMO2 + +
Mr(K)
55-
40-
35-
26-
95-
72-
17-
Ni2+ pulldown
Input
FADD-SUMO2
FADD (IB : FADD)
SENP2 (IB : Flag)
SUMO2
SENP2 (IB : Flag)
FADD (IB : FADD)
SUMO2
Tubulin
D
Flag-SENP - 5 6 7
HA-FADD + + + +
His-SUMO2 + + + +
Mr(K)
55-
40-
35-
26-
17-
Ni2+ pulldown
Input
FADD-SUMO2
FADD (IB : FADD)
SUMO2
FADD
SUMO2
SENP6
SENP7
SENP5
Tubulin

Figure 3. FADD is SUMOylated by the treatment with A23187.

(A) HeLa cells were untreated (Mock) or treated with 40 ng/ml TNFα plus 10 μg/ml cycloheximide (CHX) for 6 h, 0.1 μg/ml Fas Ligand (with 10 μg/ml cycloheximide) for 6 h, 40 μM Etoposide (Eto) and 2 μM thapsigargin (TG) for 24 h. Cell extracts were prepared and subjected to immunoblot analysis using anti-FADD antibody.

(B) HeLa cells stably expressing HA-RIP3 were left non-treated (NT) or treated with 40 ng/ml TNFα, 100 μM smac mimetic, 25 μM IDN (T/S/I) for 6 h or treated with 20 μM A23187 for 6 h, and then subjected to immunoblot analysis using anti-FADD and HA antibodies.

Figure 3

A

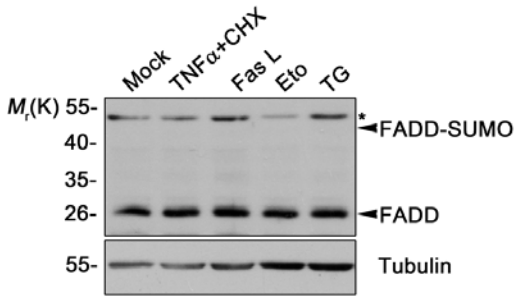
Mock
TNFα+CHX
Fas L
Eto
TG
Mr(K) 55-
40-
35-
26-
55-
*
FADD-SUMO
FADD
Tubulin

B

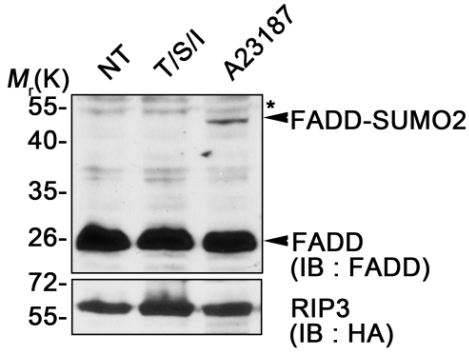
Mr(K)
NT
T/S/I
A23187
55-
40-
35-
26-
72-
55-
*
FADD-SUMO2
FADD
(IB : FADD)
RIP3
(IB : HA)

Figure 4. FADD SUMOylation occurs by A23187 in a dose- and time-dependent manner.

(A) HeLa cells were treated with the increasing concentrations of A23187 for 12 h and then subjected to immunoblot assay with FADD antibody.

(B) HeLa cells were treated with 20 μM A23187 for the indicated times. Cell lysates were subjected to immunoblot analysis with FADD, SUMO2 and Tubulin antibodies.

(C) HeLa cells were left untreated (-) or treated (+) with 20 μM A23187 for 4 h. Cell lysates were analyzed by immunoprecipitation (IP) assay with mouse IgG or FADD antibody and followed by immunoblot analysis using the indicated antibodies.

Figure 4

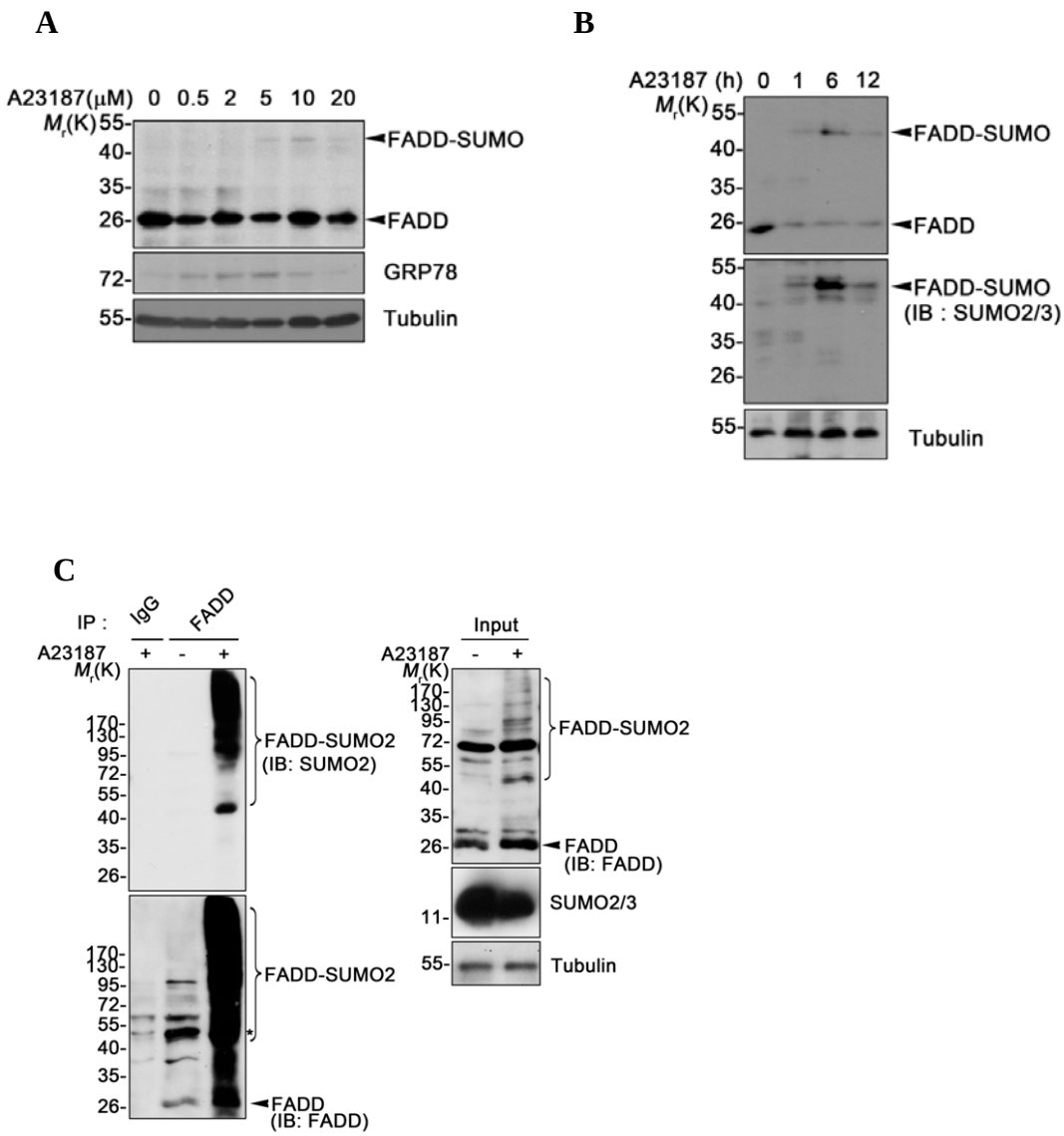
A
A23187(μM) 0 0.5 2 5 10 20
Mr(K)
55-
40-
35-
26-
FADD-SUMO
FADD
72-
GRP78
55-
Tubulin
B
A23187 (h) 0 1 6 12
Mr(K)
55-
40-
35-
26-
FADD-SUMO
FADD
55-
40-
35-
26-
FADD-SUMO
(IB : SUMO2/3)
55-
Tubulin
C
IP :
IgG
FADD
A23187
+ - +
Mr(K)
170-
130-
95-
72-
55-
40-
35-
26-
FADD-SUMO2
(IB: SUMO2)
FADD-SUMO2
FADD
(IB: FADD)
Input
A23187
- +
FADD-SUMO2
FADD
(IB: FADD)
11-
SUMO2/3
55-
Tubulin

Figure 5. FADD binds to PIAS3 in the cells exposed to A23187.

HeLa cells were incubated with 20 μM A23187 for 6 h. Cell lysate were prepared and subjected to immunoprecipitation (IP) assay with anti-FADD antibody or mouse IgG followed by immunoblotting with anti-PIAS3 or anti-FADD antibody.

Figure 5

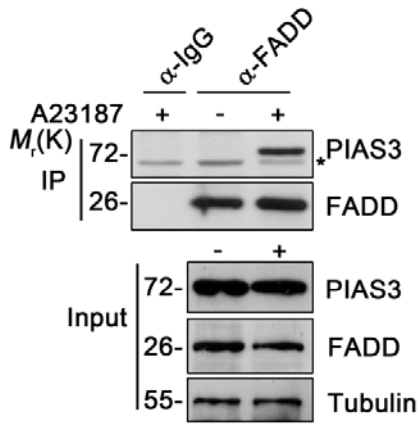
α-IgG
α-FADD
A23187
+
-
+
M_r(K)
72-
IP
26-
*PIAS3
FADD
-
+
Input
72-
PIAS3
26-
FADD
55-
Tubulin

Figure 6. FADD Lys120, 125 and 149 are the potent SUMO acceptor sites.

(A) HEK293T cells were co-transfected with HA-FADD wild-type (WT) or point mutant (lysine to arginine) at lysine 24, 33, 35, 110, 120, 125, 149, or 153 together with Flag-Ubc9 and His-SUMO2 in the presence of 25 μM IDN. After 24 h, cell lysates were subjected to Ni^{2+} pull-down assay and immunoblot analysis using anti-HA and SUMO2 antibody.

(B) Each HA-tagged FADD wild-type (WT) or double mutants at K125/149R, K120/125R or K120/149R were co-expressed with His-SUMO2 in HEK293T cells in the presence of 25 μM IDN. Cell lysates were precipitated using Ni^{2+} beads and the precipitates were analyzed by immunoblotting using anti-FADD, anti-SUMO2 and anti-Tubulin antibodies.

Figure 6

A

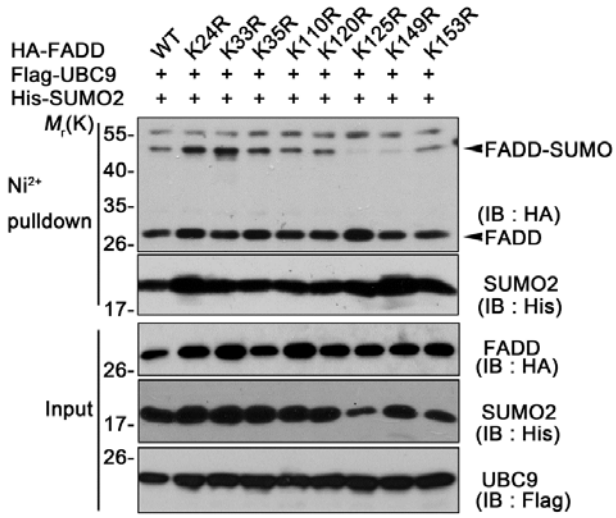
HA-FADD
Flag-UBC9
His-SUMO2
WT
K24R
K33R
K35R
K110R
K120R
K125R
K149R
K153R
M_r(K)
55-
40-
35-
26-
17-
Ni^{2+}
pulldown
FADD-SUMO
(IB : HA)
FADD
SUMO2
(IB : His)
Input
FADD
(IB : HA)
SUMO2
(IB : His)
UBC9
(IB : Flag)

B

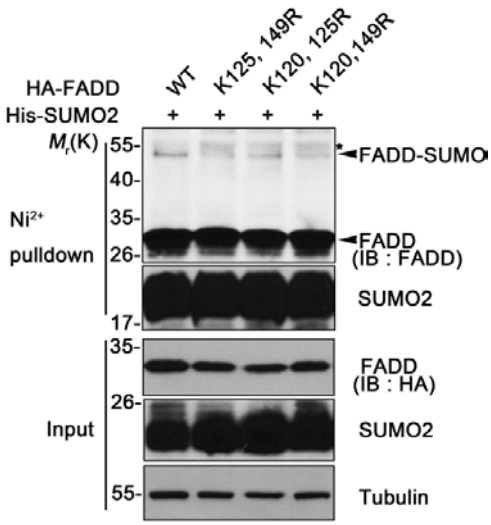
HA-FADD
His-SUMO2
WT
K125, 149R
K120, 125R
K120,149R
M_r(K)
55-
40-
35-
26-
17-
Ni^{2+}
pulldown
FADD-SUMO
FADD
(IB : FADD)
SUMO2
Input
FADD
(IB : HA)
SUMO2
Tubulin

Figure 7. Triple mutation at Lys120, 125, 149 ablates FADD SUMOylation *in vivo*.

(A) HEK293T cells were transfected with His-SUMO2 and either FADD wild-type (WT) or triple mutant at K120/125/149R (3KR) in the absence or presence of Flag-Ubc9 and 25 μM IDN for 24 h. Cell lysates were precipitated using Ni^{2+} beads and analyzed by immunoblotting using anti-FADD, anti-SUMO2 and anti-Tubulin antibodies.

(B) HeLa cells were transfected with HA-FADD wild-type (WT) or K120/125/149R (3KR) mutant in the presence of 25 μM IDN for 24 h and then exposed to 20 μM A23187 for 6 h. Cell lysates were subjected to immunoblot assay using the indicated antibodies.

Figure 7

A

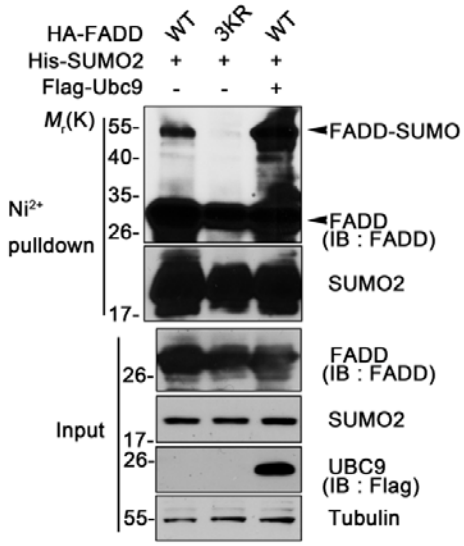
HA-FADD
WT
3KR
WT
His-SUMO2
+
+
+
Flag-Ubc9
-
-
+
M_r(K)
55-
40-
35-
26-
17-
Ni2+
pulldown
FADD-SUMO
FADD
(IB : FADD)
SUMO2
Input
26-
17-
26-
55-
FADD
(IB : FADD)
SUMO2
UBC9
(IB : Flag)
Tubulin

B

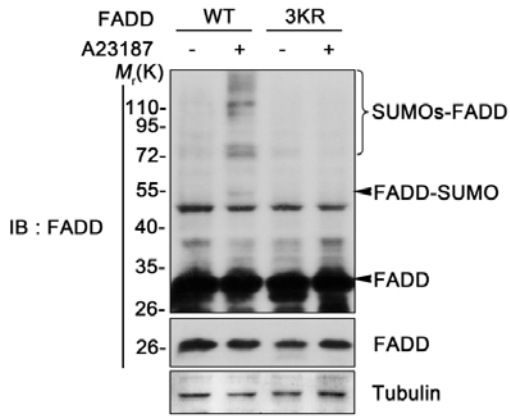
FADD
WT
3KR
A23187
-
+
-
+
M_r(K)
110-
95-
72-
55-
40-
35-
26-
26-
IB : FADD
SUMOs-FADD
FADD-SUMO
FADD
FADD
Tubulin

Figure 8. FADD accumulates onto the mitochondria following calcium overload.

(A) After treatment with either DMSO or 20 μM A23187 for 3 h, cytosolic and mitochondrial fractions were prepared and analyzed by immunoblot assay using anti-IκBα, anti-TOM20, anti-FADD, anti-Drp1 and anti-p53 antibodies.

(B) HeLa/Mito-RFP cells were treated with DMSO (vehicle) or 10 μM A23187 for 3 h and then analyzed by immunocytochemical assay. Nuclei were stained with DAPI. Scale bar. 20 μm.

(C) HeLa cells were treated with 20 μM A23187 for the indicated times and each cytosolic and mitochondrial fraction was analyzed by immunoblotting.

Figure 8

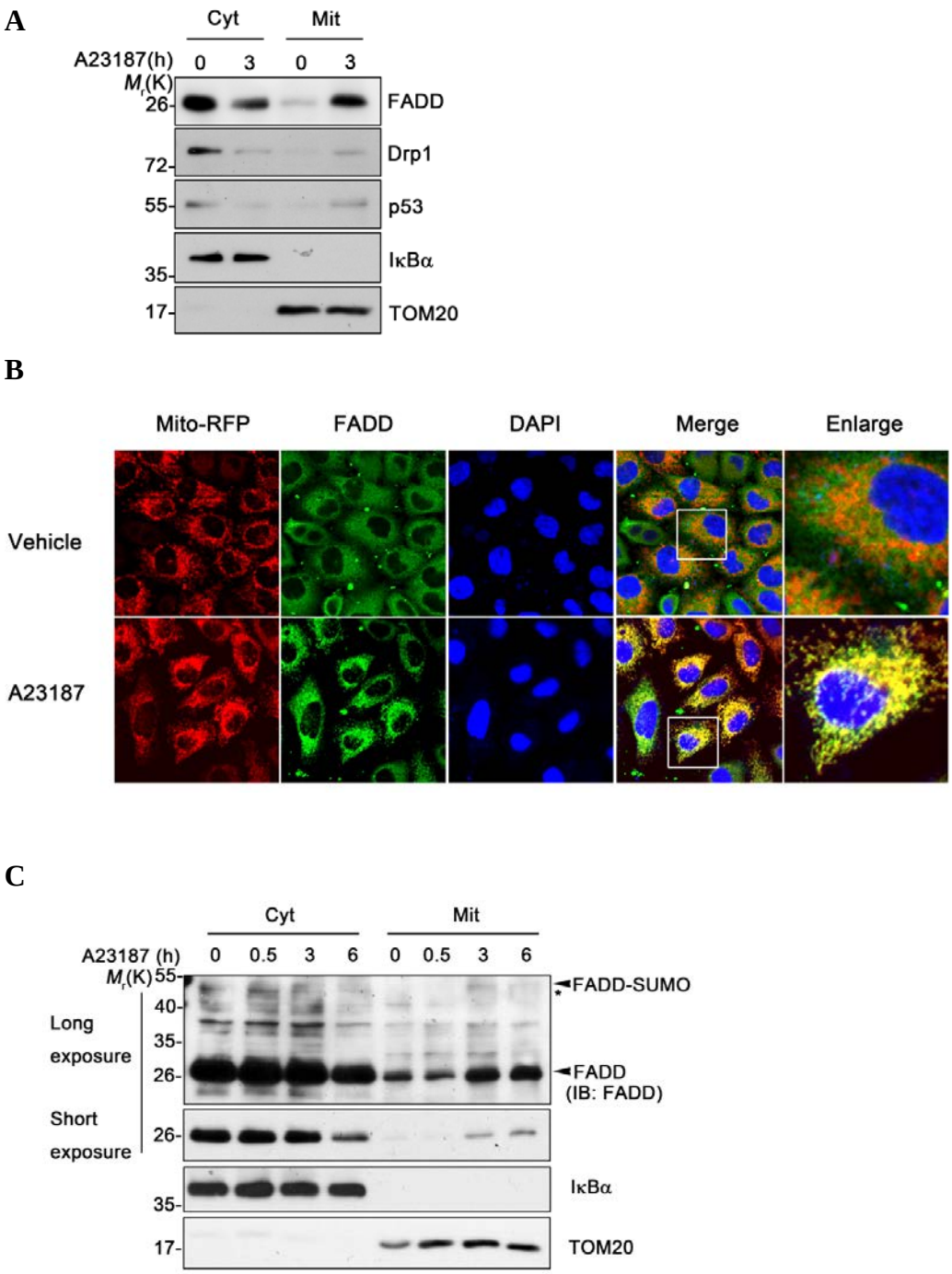
A
Cyt
Mit
A23187(h)
0
3
0
3
M_r(K)
26-
FADD
72-
Drp1
55-
p53
IκBα
35-
17-
TOM20
B
Mito-RFP
FADD
DAPI
Merge
Enlarge
Vehicle
A23187
C
Cyt
Mit
A23187 (h)
0
0.5
3
6
0
0.5
3
6
M_r(K)
55-
40-
35-
26-
Long exposure
Short exposure
FADD-SUMO
FADD (IB: FADD)
IκBα
TOM20

Figure 9. FADD deficiency does not affect mPTP formation.

(A and B) Wild-type (WT) and FADD knockout ($FADD^{-/-}$) MEFs were treated with 20 μM A23187 for 3 h, and then analyzed by calcein release assay. Representative images are shown by confocal microscopy (A). Calcein fluorescence in the images of Fig. (A) was measured by Image J program (B). Bars represent mean values ± S.D. of the fluorescence from three independent experiments.

Figure 9

A

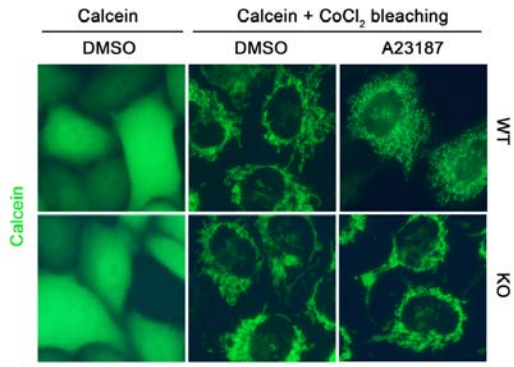
Calcein
Calcein + CoCl2 bleaching
DMSO
DMSO
A23187
Calcein
WT
KO

B

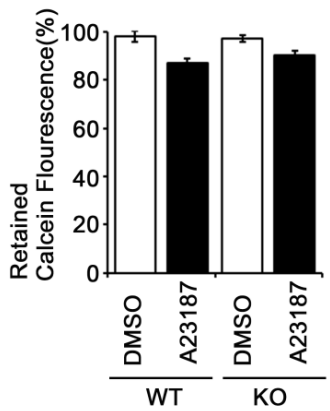
Retained
Calcein Flourescence(%)
100
80
60
40
20
0
DMSO
A23187
DMSO
A23187
WT
KO

Figure 10. FADD- or Drp1-deficient MEFs are resistant to A23187-induced mitochondrial fragmentation.

(A and B) Wild-type (WT), $FADD^{-/-}$ and $Drp1^{-/-}$ MEFs were transfected with mito-GFP for 24 h and left untreated (DMSO) or treated with 20 μM A23187 for 3 h. Representative images were obtained by fluorescence microscopy (A). Mitochondrial fragmentation ratios were determined by counting the cells showing fragmented mitochondria among total GFP-positive cells (Each group > 100 cells) (B). Bars represent mean values ± S.D. (n = 3). *P < 0.05, **P < 0.01.

Figure 10

A

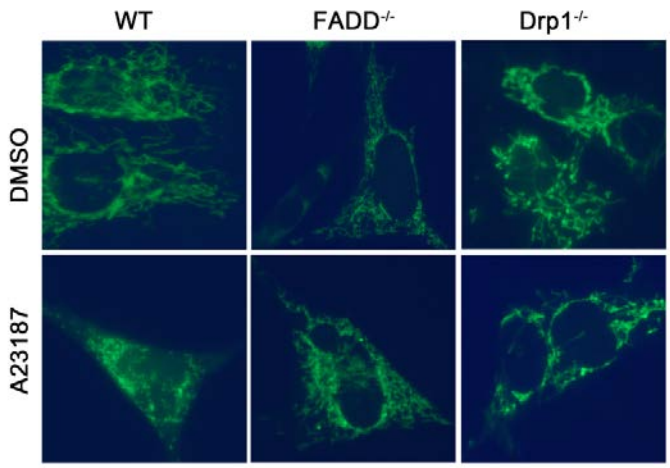
WT
FADD-/-
Drp1-/-
DMSO
A23187

B

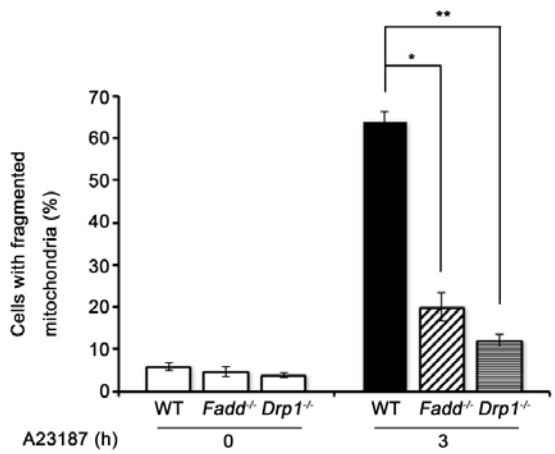
**
*
70
60
50
40
30
20
10
0
Cells with fragmented mitochondria (%)
WT
Fadd-/-
Drp1-/-
WT
Fadd-/-
Drp1-/-
A23187 (h)
0
3

Figure 11. SUMO-defective FADD mutant suppresses A23187-induced mitochondrial fragmentation.

HeLa cells stably expressing mito-RFP were transfected with pcDNA (EV), HA-FADD wild-type (WT) or K120/125/149R mutant (3KR) for 24 h and then exposed with 10 μM A23187 for 3 h. Percentage of GFP-positive cells showing mitochondrial fragmentation among total RFP-positive cells were determined under fluorescence microscope (Each group > 100 cells). Bars indicate mean values ± S.D. (n = 3). *P < 0.05, **P < 0.01.

Figure 11

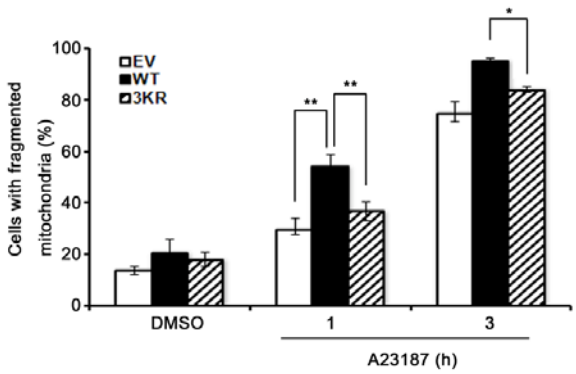
Cells with fragmented mitochondria (%)
100
80
60
40
20
0
EV
WT
3KR
**
**
*
DMSO
1
3
A23187 (h)

Figure 12. Dominant-negative form of Drp1 prevents FADD-mediated mitochondrial fragmentation.

Mito-RFP-expressing HeLa cells were co-transfected with Drp1 K38A and either FADD wild-type (WT) or K120/125/149R (3KR) mutant in the presence of 25 μM IDN. After 24 h, cells were incubated with 10 μM A23187 for 1 h. Expression levels of FADD and Drp1 were examined by immunoblot assay (bottom). Percentage of GFP-positive cells showing mitochondria fragmentation among total RFP-positive cells were determined under fluorescence microscope (Each group > 100 cells). Bars indicate mean values ± S.D. (n = 3). ** $P < 0.01$.

Figure 12

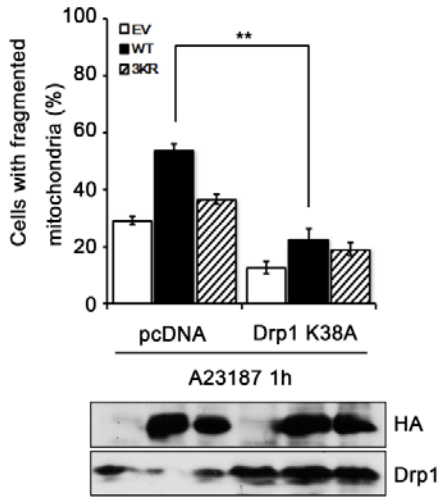
100
80
60
40
20
0
EV
WT
3KR
**
Cells with fragmented mitochondria (%)
pcDNA
Drp1 K38A
A23187 1h
HA
Drp1

Figure 13. A23187 induces the interaction of FADD with Drp1 in the cytoplasm and mitochondria.

HeLa cells were left untreated or treated with 20 μM A23187 for 3 h and cell lysates were analyzed by immunoprecipitation (IP) assay using IgG or anti-FADD antibody followed by immunoblot analysis using the indicated antibodies (upper). Whole cell lysates (input) were examined by immunoblotting (lower).

Figure 13

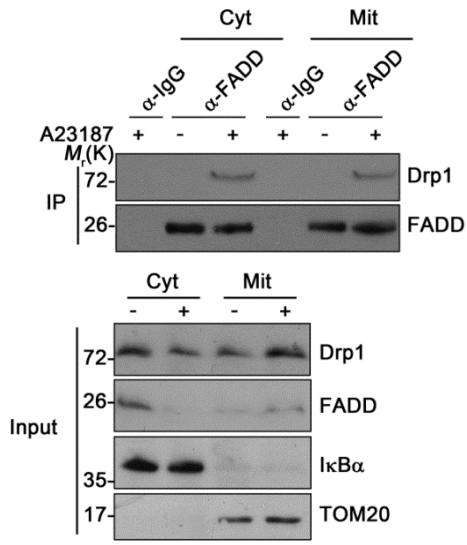
Cyt
Mit
α-IgG
α-FADD
α-IgG
α-FADD
A23187 + - + + - +
Mr(K)
IP
72-
26-
Drp1
FADD
Cyt
Mit
- + - +
Input
72-
26-
35-
17-
Drp1
FADD
IκBα
TOM20

Figure 14. SUMOylated FADD interacts with Drp1 *in vitro* and in cells.

(A) HeLa cells were transfected with HA-FADD wild-type (WT) or K120/125/149R (3KR) mutant in the presence of 25 μM IDN for 24 h and then treated with 10 μM A23187 for 1 h. Cytosolic and mitochondrial fractions were prepared by fractionation assay and analyzed by immunoprecipitation (IP) assay using anti-HA antibody. The immunoprecipitants and whole cell lysates (Input) were analyzed by immunoblotting using the indicated antibodies.

(B) Purified Myc-Drp1 protein (1 μg) was incubated with *in vitro* SUMOylated His-FADD or native His-FADD protein followed by immunoprecipitation (IP) assay using anti-Drp1 antibody. The immunoprecipitates and reaction proteins were analyzed by western blotting.

Figure 14

A

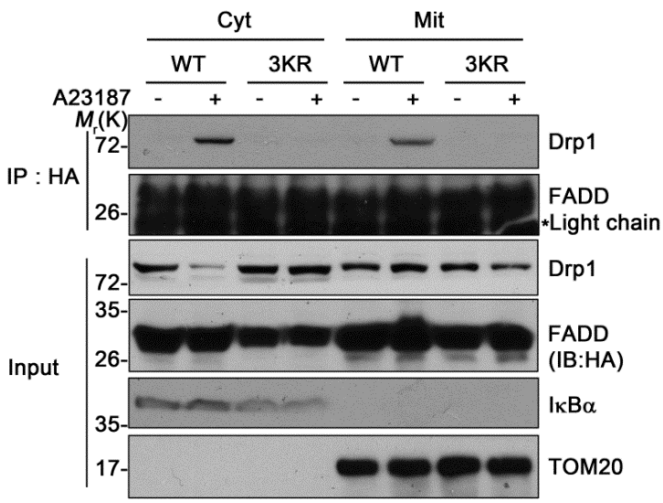
Cyt
Mit
WT
3KR
WT
3KR
A23187
- + - + - + - +
M_r(K)
IP : HA
72-
26-
Drp1
FADD
*Light chain
Input
72-
35-
26-
35-
17-
Drp1
FADD
(IB:HA)
IκBα
TOM20

B

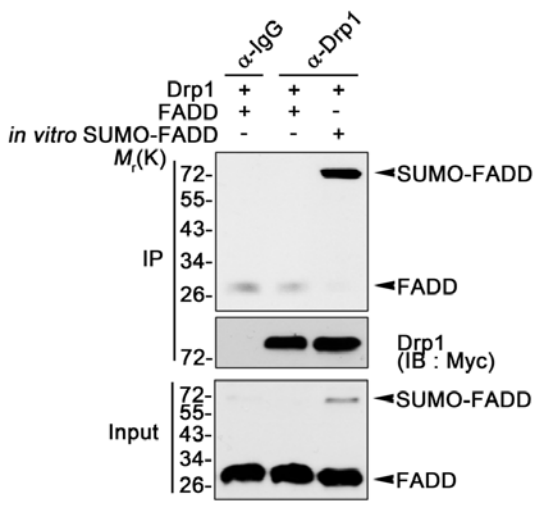
α-IgG
α-Drp1
Drp1 + + +
FADD + + -
in vitro SUMO-FADD - - +
M_r(K)
IP
72-
55-
43-
34-
26-
72-
SUMO-FADD
FADD
Drp1
(IB : Myc)
Input
72-
55-
43-
34-
26-
SUMO-FADD
FADD

Figure 15. FADD is required for A23187-induced Drp1 translocation onto the mitochondria and interacts with Mff.

(A) HeLa cells were co-transfected with HA-FADD and either GFP-Fis1, GFP-Mff, GFP-MiD49 or GFP-MiD51 in the presence of 25 μM IDN for 24 h. After treatment with 20 μM A23187 for 3 h, cytosolic and mitochondrial fractions were prepared and subjected to immunoprecipitation (IP) assay using anti-HA antibody. The immunoprecipitates and whole cell lysates (Input) were analyzed by immunoblotting with the indicated antibodies.

(B) FADD wild-type (WT) or knock-out (KO) MEFs were treated with 20 μM A23187 for 3 h. Cell lysates were fractionated into cytosolic and mitochondrial fractions and the fractions were analyzed by immunoblot assay using the indicated antibodies.

Figure 15

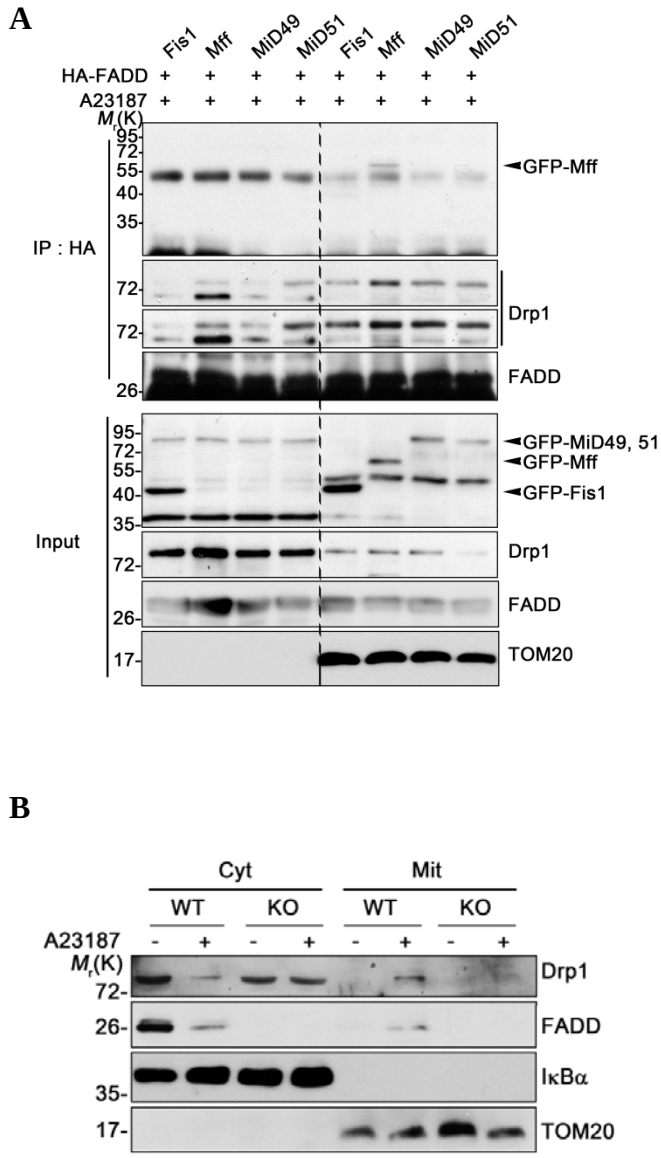
A
Fis1
Mff
MiD49
MiD51
Fis1
Mff
MiD49
MiD51
HA-FADD + + + + + + + +
A23187 + + + + + + + +
Mr(K)
95-
72-
55-
40-
35-
GFP-Mff
IP : HA
72-
Drp1
72-
FADD
26-
95-
72-
55-
40-
35-
GFP-MiD49, 51
GFP-Mff
GFP-Fis1
Input
Drp1
72-
FADD
26-
TOM20
17-
B
Cyt
Mit
WT
KO
WT
KO
A23187 - + - + - + - +
Mr(K)
72-
Drp1
26-
FADD
IκBα
35-
17-
TOM20

Figure 16. High dose of A23187 triggers caspase-independent cell death.

(A) HeLa cells were exposed to 2 μM or 5 μM A23187 for the indicated times in the presence or absence of 25 μM IDN and cell death rates were determined by counting the numbers of propidium iodide (PI)-positive cells among total cells after staining with PI. Bars indicate mean values ± S.D. (*n* = 3).

(B) HeLa cells were treated with 20 μM A23187 or 40 ng/ml TNFα plus 1 μg/ml cycloheximide (CHX) and cell lysates were subjected to immunoblot assay using anti-caspase9 (Casp9), anti-caspase-8 (Casp8) and anti-Tubulin antibodies.

(C) HeLa cells were treated with 20 μM A23187 for 5 h or 40 ng/ml TNFα plus 1 μg/ml cycloheximide (CHX) for 12 h and their cytosolic and mitochondrial fractions were analyzed by immunoblotting using anti-cytochrome *c*, anti-IκBα and anti-TOM20 antibodies.

Figure 16

A

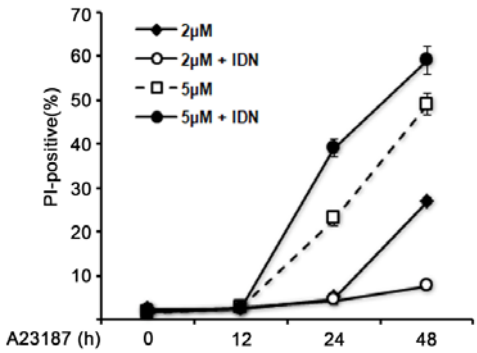

B

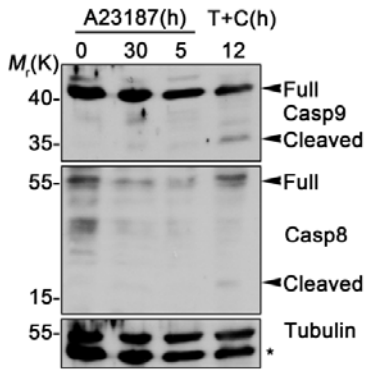

C

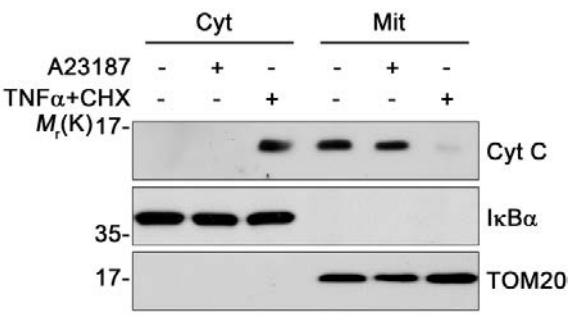

Figure 17. Deficiency of FADD or Drp1 and expression of FADD 3KR mutant suppress A23187-induced necrosis.

(A) FADD wild-type (WT), FADD knock-out ($FADD^{-/-}$) and Drp1 knock-out ($Drp1^{-/-}$) MEFs were treated with 20 μM A23187 for the indicated times and cell death rates were measured by counting the number of propidium iodide (PI)-positive cells. Bars indicate mean values ± S.D. (n = 3) (upper).

(B) HeLa cells were pre-treated with 25 μM IDN for 3 h and then co-transfected with EGFP and FADD wild-type (WT) or K120/125/149R (3KR) mutant in the presence of 25 μM IDN for 24 h. After treatment with 20 μM A23187 for the indicated times, cell death rates were measured as described in (A). Bars indicate mean values ± S.D. (n = 3). P-values were estimated using t-test versus empty control (*P < 0.05, **P < 0.01).

Figure 17

A

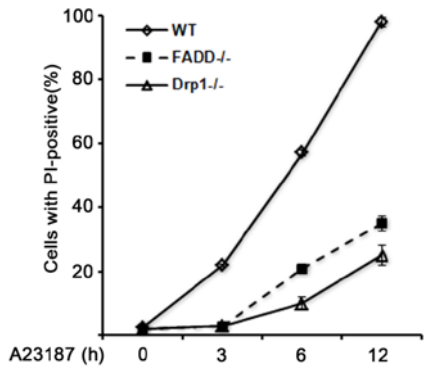
WT
FADD-/-
Drp1-/-
Cells with PI-positive(%)
100
80
60
40
20
A23187 (h)
0
3
6
12

B

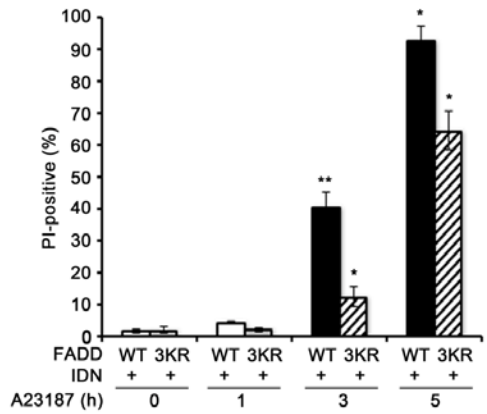
PI-positive (%)
100
90
80
70
60
50
40
30
20
10
0
FADD WT 3KR WT 3KR WT 3KR WT 3KR
IDN + + + + + + + +
A23187 (h) 0 1 3 5

Figure 18. Hypoxia-induced intracellular calcium overload triggers FADD SUMOylation and translocalization onto the mitochondria.

(A) HeLa cells were exposed to normoxic (20% O_2) or hypoxic (1% O_2) conditions in the presence or absence of 10 μM BAPTA-AM for the indicated periods. Cell extracts were analyzed by western blotting.

(B) HeLa cells were cultivated under hypoxic condition (1% O_2) for 24 h and then under reoxygenation (Reox) for 2 and 4 h. The cell lysates were analyzed by western blotting.

(C) HeLa cells were incubated under hypoxic condition for the indicated times and cytosolic and mitochondrial fractions were prepared and analyzed by western blotting using the indicated antibodies.

Figure 18

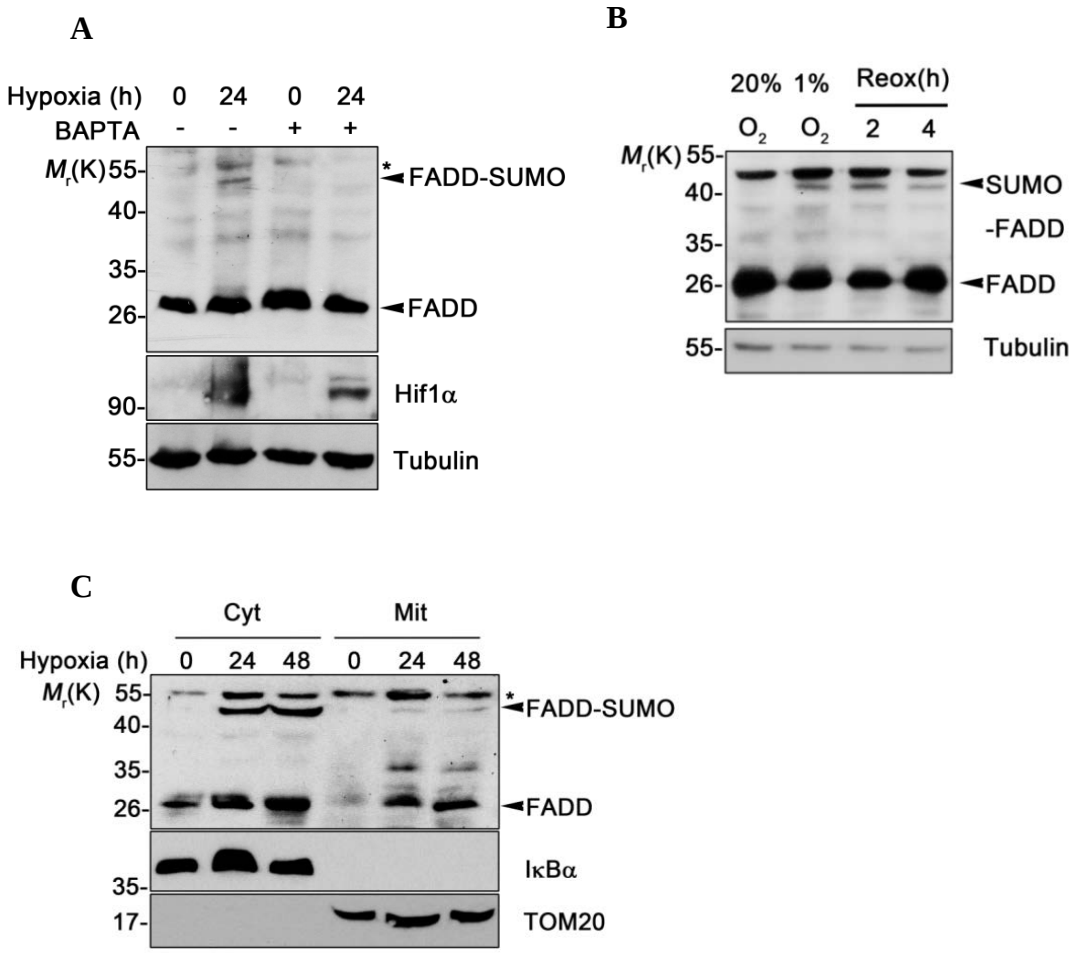
A
Hypoxia (h) 0 24 0 24
BAPTA - - + +
M_r(K) 55-
40-
35-
26-
90-
55-
*FADD-SUMO
FADD
Hif1α
Tubulin
B
20% 1% Reox(h)
O_2 O_2 2 4
M_r(K) 55-
40-
35-
26-
55-
SUMO
-FADD
FADD
Tubulin
C
Cyt Mit
Hypoxia (h) 0 24 48 0 24 48
M_r(K) 55-
40-
35-
26-
35-
17-
*FADD-SUMO
FADD
IκBα
TOM20

Figure 19. Knockdown of FADD expression suppress hypoxia-induced necrotic cell death.

HeLa cells were transfected with GFP and either pSUPER.neo (EV) or FADD shRNA (shFADD) for 48 h. Cells were then exposed to hypoxia in the presence or absence of 25 μM IDN. After staining with propidium iodide (PI), cell death rates were measured as described in Fig. 17B. Bars indicate mean values ± S.D. (n = 3). **P < 0.01, ***P < 0.001.

Figure 19

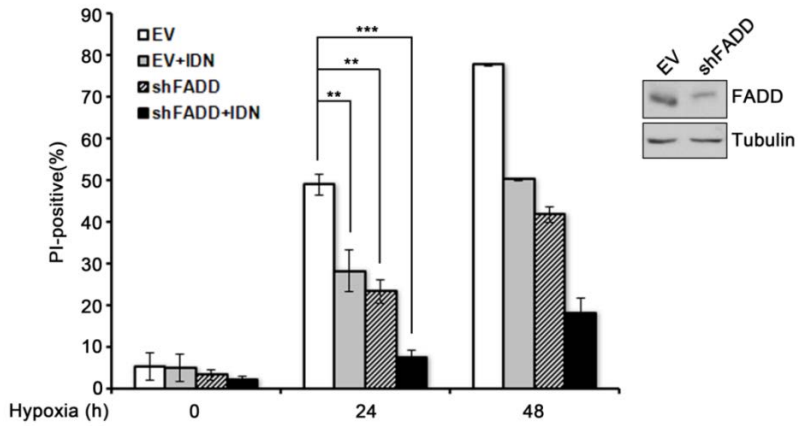
EV
EV+IDN
shFADD
shFADD+IDN
PI-positive(%)
Hypoxia (h)
0
24
48
***
**
**
EV
shFADD
FADD
Tubulin

Figure 20. SUMOylated FADD interacts with Drp1 in the brain of ischemic stroke.

(A and B) Wild-type (WT) mice (3-month-old male, BALB/c) were subject to tMCAO for 30 min. The brain lysates (except cerebellum) were then prepared from non-ischemic (contralateral, C), ischemic (ipsilateral, I) and sham control (S) hemispheres and subjected to (A) immunoblotting using the indicated antibodies (A) or immunoprecipitation assay using anti-FADD antibody. The immunoprecipitates and whole cell lysates (Input) were analyzed by immunoblotting (B).

Figure 20

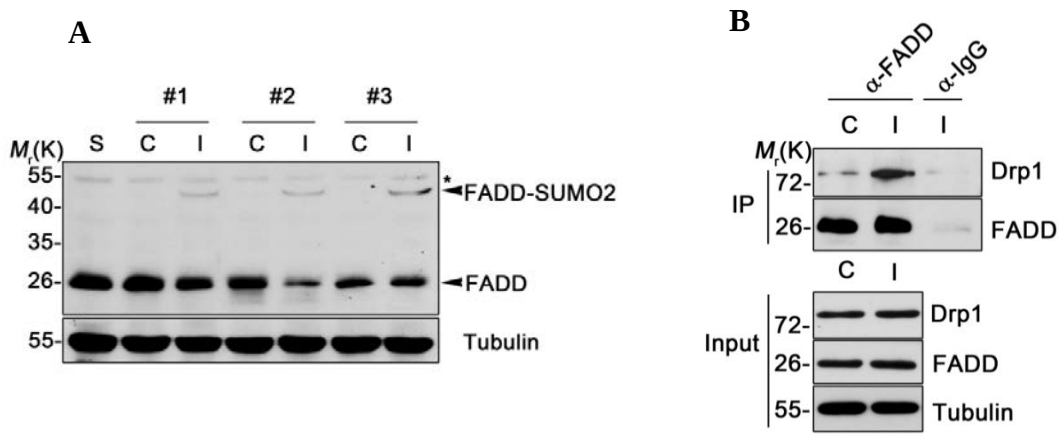
A
#1
#2
#3
M_r(K)
S
C
I
C
I
C
I
55-
40-
35-
26-
55-
*
FADD-SUMO2
FADD
Tubulin
B
α-FADD
α-IgG
C
I
I
M_r(K)
IP
72-
26-
Drp1
FADD
C
I
Input
72-
26-
55-
Drp1
FADD
Tubulin

Figure 21. Knockdown of Casepase-10 expression prevents A23187-induced mitochondrial fragmentation.

(A) Mito-RFP-expressing HeLa cells were transfected with FADD-, Caspase-8- or Caspase-10-targeting shRNA or with Drp1 K38A mutant together with eGFP. After 48 h, cells were treated with 10 μM A23187 for 2 h. Mitochondria morphology in GFP-positive cells was analyzed by fluorescence microscopy (upper). Cell extracts were analyzed by immunoblotting using the indicated antibodies (lower).

(B) Mitochondrial fragmentation was determined by the ratios of GFP-positive cells showing fragmented mitochondria among total GFP-positive cells. Each group counted at least 100 cells. Bars indicate mean values ± S.D. (n = 3).

Figure 21

A

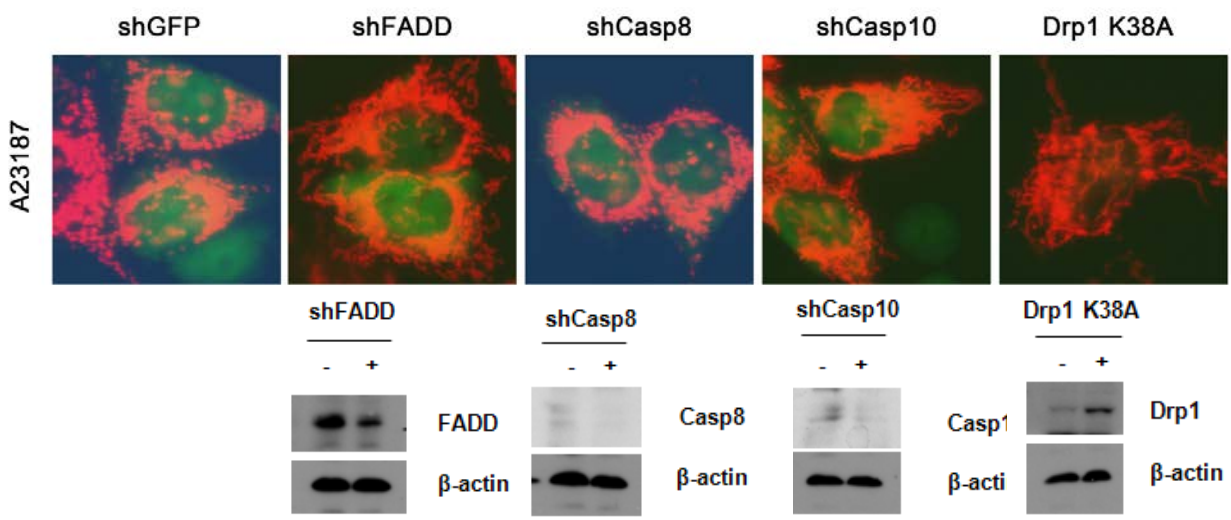
shGFP
shFADD
shCasp8
shCasp10
Drp1 K38A
A23187
shFADD
shCasp8
shCasp10
Drp1 K38A
- +
- +
- +
- +
FADD
β-actin
Casp8
β-actin
Casp1
β-acti
Drp1
β-actin

B

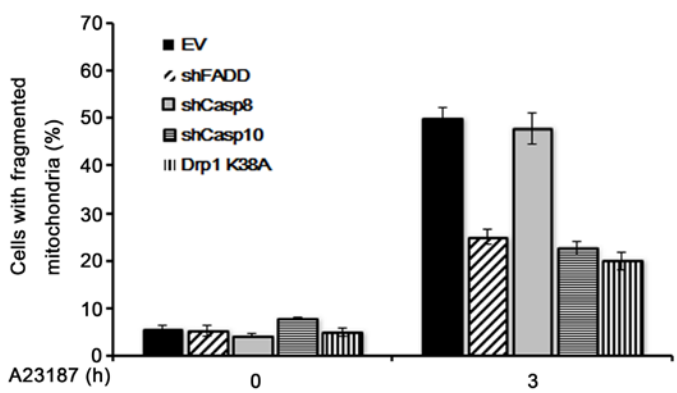
Cells with fragmented mitochondria (%)
70
60
50
40
30
20
10
0
EV
shFADD
shCasp8
shCasp10
Drp1 K38A
A23187 (h)
0
3

Figure 22. Caspase-10 forms a protein complex with FADD and Drp1 in the mitochondrial fraction upon A23187 treatment.

(A) FADD wild-type ($FADD^{+/+}$) or knock-out ($FADD^{-/-}$) MEFs were transfected with Caspase-10 for 24 h and then treated with 20 μM A23187 for 3 h. Cell lysates were subjected to immunoprecipitation (IP) assay using anti-Drp1 antibody. The immunoprecipitants and whole cell lysates (Input) were analyzed by immunoblotting using the indicated antibodies.

(B) HeLa cells were transfected with FADD-HA for 24 h cells and then treated with 20 μM A23187 for 3 h. Cytosolic and mitochondrial fractions were prepared and subjected to immunoprecipitation (IP) assay using anti-FADD antibody following by immunoblot assay.

Figure 22

A

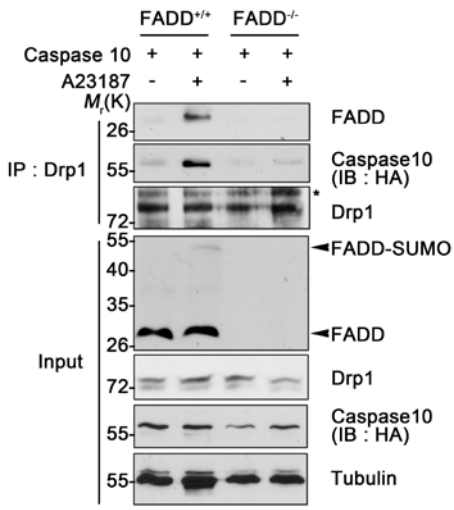
FADD+/+
FADD-/-
Caspase 10 + + + +
A23187 - + - +
Mr(K)
IP : Drp1
26-
55-
72-
FADD
Caspase10 (IB : HA)
*
Drp1
Input
55-
40-
35-
26-
72-
55-
55-
FADD-SUMO
FADD
Drp1
Caspase10 (IB : HA)
Tubulin

B

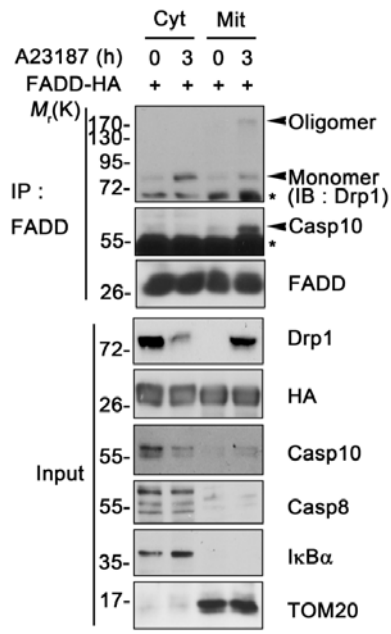
Cyt
Mit
A23187 (h) 0 3 0 3
FADD-HA + + + +
Mr(K)
IP : FADD
170-
130-
95-
72-
55-
26-
Oligomer
Monomer (IB : Drp1)
*
Casp10
*
FADD
Input
72-
26-
55-
55-
35-
17-
Drp1
HA
Casp10
Casp8
IκBα
TOM20

Figure 23. Familial mutation L248F of Caspase-10 enhances A23187-induced necrotic cell death and mitochondrial fragmentation.

(A and B) MCF7 cells were transfected with GFP and pcDNA (-), Caspase-10 wild-type (WT), V410I or L285F mutant for 24 h. Cells were then treated with 25 ng/ml TRAIL for 8 h (A) or 20 μM A23187 (B) for the indicated times. After staining with propidium iodide (PI), cell death rates were determined as in Fig. 17B. Bars indicate mean values ± S.D. (n = 3).

(C) MCF7 cells were transfected with mito-RFP and pcDNA (-), Caspase-10 wild-type (WT), V410I or L285F mutant for 24 h. Mitochondrial fragmentation was examined by counting RFP-positive cells showing fragmented mitochondria among total RFP-positive cells. Each group counted at least 100 cells. Values indicate mean values ± S.D. (n = 3).

Figure 23

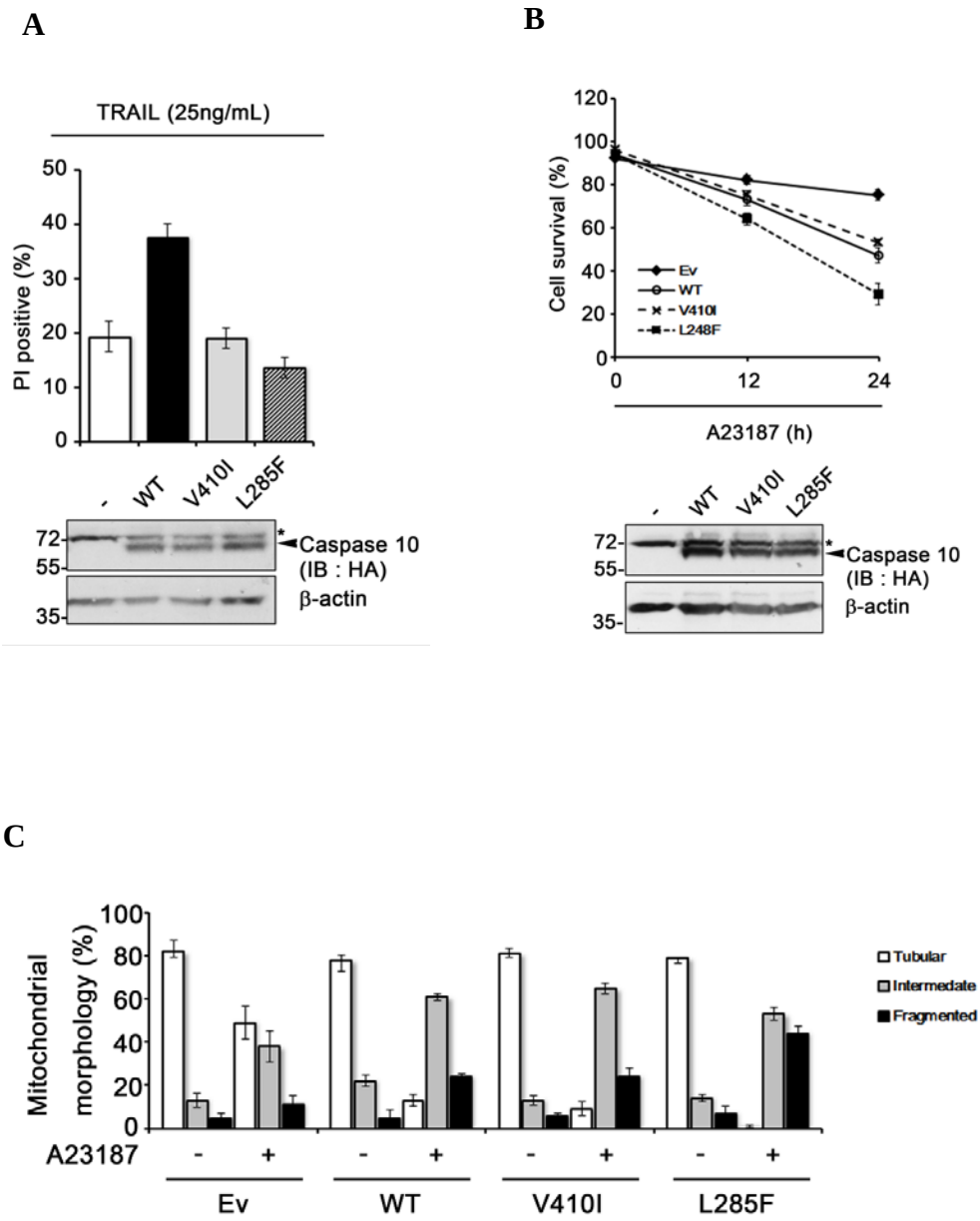
A
TRAIL (25ng/mL)
PI positive (%)
50
40
30
20
10
0
-
WT
V410I
L285F
72
55
35
Caspase 10
(IB : HA)
β-actin
B
Cell survival (%)
120
100
80
60
40
20
0
Ev
WT
V410I
L248F
0
12
24
A23187 (h)
-
WT
V410I
L285F
72
55
35
Caspase 10
(IB : HA)
β-actin
C
Mitochondrial morphology (%)
100
80
60
40
20
0
Tubular
Intermedate
Fragmented
A23187
-
+
-
+
-
+
-
+
Ev
WT
V410I
L285F

Figure 24. Caspase-10 accelerates Drp1 oligomerization during A23187 treatment.

MCF7 cells were transfected with GFP and pcDNA (-), Caspase-10 wild-type (WT), V410I (VI) and Death effector domain (DED) for 24 h in the presence of 25 μM IDN. Cells were treated with 20 μM A23187 for 12 h, lyzed in non-reducing condition and subjected to immunoblot assay using the indicated antibodies.

Figure 24

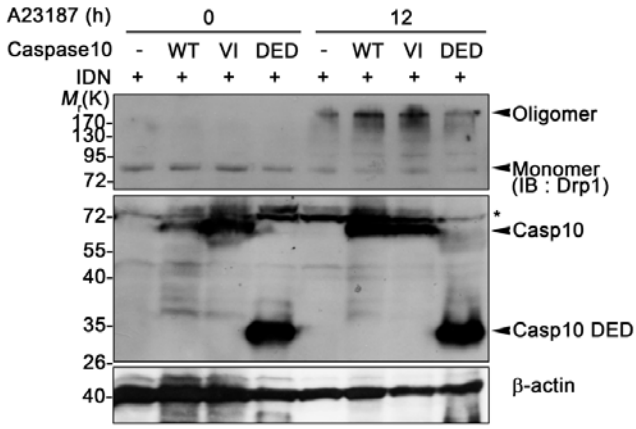
A23187 (h)
0
12
Caspase10
-
WT
VI
DED
-
WT
VI
DED
IDN
+
+
+
+
+
+
+
+
M_r(K)
170
130
95
72
72
55
40
35
26
40
Oligomer
Monomer
(IB : Drp1)
*
Casp10
Casp10 DED
β-actin

Discussion

Most of SUMOylation occur at the consensus motif (ΨKxD/E) in target protein substrates and this prospectiveness is due to being of a single E2 enzyme (UBC9) which interacts with the consensus motif for SUMO conjugation (37). According to our observations, the three lysine residues (Lys120, Lys125 and Lys149) in the death domain of FADD contribute to its SUMO modification because mutation in all of these three lysines only can abolish SUMOylation. Interestingly, the sequences surrounding the three lysines in FADD, $_{119}$LKVS$_{122}$, $_{124}$TKID$_{127}$, $_{148}$WKNT$_{151}$, are not in the consensus with the canonical SUMOylation motif. Recent evidences extend this simple consensus SUMO-acceptor motif to two additional exceptions, the phosphorylation-dependent SUMOylation motif (PDSM) and the negatively charged amino acid-dependent SUMOylation motif (NDSM) (Gareau and Lima 2010). While a phosphorylation at 198 serine residue in human FADD occurs upon signaling, FADD phospho-mimic or -dead mutant is also conjugated with SUMO2 (data not shown). Thus, the three lysine residues in FADD do not coincide with the PDSM either. In addition, some of the SUMO-acceptor lysines have also been identified

that do not coincide with the consensus motif (Miyauchi et al. 2002; Lee et al. 2003; Blomster et al. 2010; Smith et al. 2011). For instance, the lysine14-containing SUMO-acceptor site in human ubiquitin conjugation enzyme E2-25K ($_{13}$FKEW$_{16}$) does not require these acidic residues for its SUMOylation but is recognized in the context of stable α-helix (Pichler et al. 2005). Similarly, the three lysine residues in FADD are a part of α-helix and are closely proximate in the secondary structure. However, the detailed study on the motif requires further study.

Among the regulations by SUMOylation, altered functions in apoptosis were reported in a few cases (Buschmann et al. 2000; Babic et al. 2006; Meinecke et al. 2007). Especially, a recent report showed that FADD, a main adaptor protein transmitting DR-mediated apoptosis, also participates as a negative regulator after ubiquitination in the necroptosis (Lee et al. 2012). On the other hand, I found that FADD did not undergo SUMOylation during apoptosis or necroptosis (Fig. 3A and 3B). Instead, I found that Ca^{2+}-overload triggers other type of regulated necrosis, which is distinct from either apoptosis triggered by low level of calcium or necroptosis. This type of necrotic cell death initiated by Ca^{2+} overload is not dependent on caspase activation but on FADD-SUMOylation and can be found in many pathophysiologic conditions, such as a transgenic mouse

model of Huntinton's disease, cerulein-induced pancreatitis and ischemia/reperfusion (Yu et al. 2000; Orabi et al. 2010; Chen et al. 2011) . I need to expend the characterization of this type of regulated necrosis accompanying Ca^{2+} overload and FADD- SUMOylation.

Drp1-mediated mitochondrial fragmentation is a widespread phenomenon observed in the proceeding apoptosis and necrosis. In the case of apoptosis, Drp1-induced fission is related to mitochondrial outer membrane permeabilization, cristae disorganization, cytochrome *c* release and caspase activation. For necrosis, unbalanced fission led to ATP depletion, cluster around nuclei and subsequent plasma membrane destruction, nuclear membrane breakdown and cell rupture. Nevertheless, mitochondrial fragmentation-induced necrosis is poorly understood. Our results have uncovered a new mechanism in the regulated necrosis, implicating a role of SUMOylated FADD in the Drp1-mediated mitochondrial fragmentation during Ca^{2+}-overload response. This proposal is highlighted by the findings that SUMOylated FADD physically interacts with Drp1 in the cytoplasm and the resulting FADD/Drp1 complex translocates onto the mitochondria through utilizing Mff, leading to robust mitochondrial fragmentation. Thus, FADD/Drp1-induced mitochondrial damage does not accompany with any release of cytochrome c and

provokes caspase-independent necrosis. Furthermore, the observation that deficiency of FADD abolishes the translocation of Drp1 to the mitochondria for subsequent mitochondrial fragmentation and necrotic cell death enhances our understanding on the mechanism how Drp1 is recruited into the mitochondria during the necrosis.

I propose here that under Ca^{2+}-overload condition, Drp1-dependent necrosis is under the control of FADD. Recent evidence showed that Drp1 stabilize the p53 on the mitochondria to trigger necrosis and also mitochondrial p53 triggers necrosis through opening mitochondrial permeability transition pore under ischemia/reperfusion (Guo et al. 2014). However, the correlation between mitochondrial fragmentation and MPTP formation has been a subject of debate. According to our results, following the treatment with high dose of A23187, not only FADD but p53 is also accumulated on the mitochondria. Although A23187-induced Ca^{2+} overload might bring out p53 translocation or stabilization, I observed that the opening of MPTP was barely affected by A23187 (Fig. 9A and 9B). A study of Hamahata *et al*. demonstrated that A23187-induced cytoplasmic Ca^{2+} overload triggers necrotic cell death in CEM cells, a T-lymphocyte cell line, and this cell death is not affected by cyclosporin A, an MPTP inhibitor (Hamahata et al. 2005). Therefore, this discrepancy may be due to

different cell types or distinct cellular context showing different sensitivity to mitochondrial damage, remaining to be further addressed.

According to paradigm of ischemic stroke, ischemic core in which brain regions sustain severely impaired blood flow undergoes necrotic cell death rather than apoptosis. On the other hand, ischemic penumbra lying between ischemic core and normal brain tissue preserves partially bioenergetic processes but is functionally impaired and prone to occurring apoptosis (Markus et al. 2004). In the ischemic core, reduced ATP production increases intracellular calcium levels by opening two glutamate ionotropic receptors, NMDA receptor and AMPA receptor, to trigger necrotic cell death in neurons. In the MCAO model, I also observed FADD SUMOylation in the ipsilateral cortex (Fig. 20A) and its interaction with Drp1 (Fig. 20B). In addition, the increase of hypoxic damage well correlates with the enhanced level of FADD SUMOylation. In non-excitable HeLa cells, hypoxia-induced calcium influx is unclear but I found that hypoxia-induced cell death was suppressed by calcium chelator (Fig. 18A). Future challenge is to investigate FADD SUMOylation in and a role of SUMOylated FADD in other types of necrotic cell death, such as myocardial infarction or neurodegenerative disorders. Based on the findings in this study, I propose a model for the role of FADD

SUMOylation in calcium-overload induced necrotic cell death (Fig. 25).

In summary, I show a novel mechanism underlying new type of regulated necrosis utilizing SUMOylated FADD that regulates Drp1-mediated mitochondrial fragmentation. Especially, FADD SUMOylation is crucial for mitochondrial and cellular damages under calcium-overload and hypoxia-ischemia, providing insight into developing new therapeutic opportunity.

Figure 25. A proposed role of FADD SUMOylation in calcium overload-induced necrotic cell death. FADD is SUMOylated by calcium-overload and SUMOylated FADD binds to Drp1 and functions to recruit Drp1 to the mitochondria. Caspase-10 then binds to this SUMO-FADD/Drp1 complex on the mitochondria and promotes Drp1 oligomerization for mitochondria fragmentation and necrotic cell death.

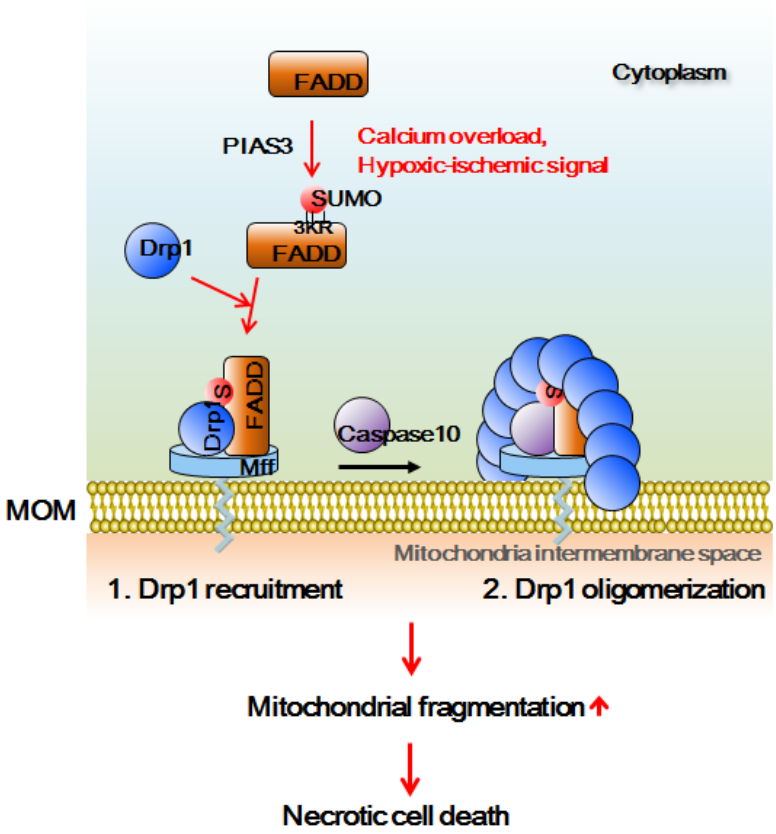
FADD
Cytoplasm
PIAS3
Calcium overload,
Hypoxic-ischemic signal
SUMO
3KR
FADD
Drp1
S
FADD
Drp1
Mff
Caspase10
MOM
Mitochondria intermembrane space
1. Drp1 recruitment
2. Drp1 oligomerization
Mitochondrial fragmentation
Necrotic cell death

Materials and Methods

Cell culture and antibodies

HeLa, HEK293T, or HT22 cells (The American Type Culture Collection (ATCC), Manassas, VA, USA) and MEFs were cultured in Dulbecco's Modified Eagles Medium (DMEM; HyClone, South Logan, UT, USA) supplemented with 10% fetal bovine serum (FBS; Hyclone). DRP1 wild-type and knockout MEFs were kind gifts from K Mihara (Kyushu University, Fukuoka, Japan). Antibodies against FADD (G-4), FADD (H-181), Drp1 (H-300) TOM20 (F-1), TOM20 (F-145), p53 (DO-1), anti-GFP (FL), anti-cytochrome C (6H2), β-actin (C4) were purchased from Santa Cruz (Santa Cruz Biotechnology, CA, USA). Anti-Xpress (Invitrogen; 1405573), anti-α-tubulin (Sigma-Aldrich, St Louis, MO, USA), anti-Flag (Sigma-Aldrich; F1804), anti-SUMO-2 (Zymed Laboratories), anti-PIAS3 (Cell Signaling), anti-Xpress (Invitrogen), anti-His (BD Biosciences), IκBα (cell signaling), anti-caspase-9 (Cell Signaling, Danvers, MA, USA; #9502) anti-Hif1α (Caymen; 10006461), and anti-caspase-8 antibodies were used in immunoblot analysis. Transfection was carried out with LipofectAMINE (Invitrogen), Polyfect reagent (Qiagen, Valencia, CA, USA) or PEI (Sigma) following the manufacturer's instructions. Typically, 2

× 10^5 cells per well in 6-well dishes were transfected with appropriate plasmids.

Plasmid construction and site-directed mutagenesis

pcDNA-HA-FADD have previously described (5). FADD cDNA was cloned into pET-28a for bacterial expression. The SUMO-1, SUMO-2, Ubc9, SENPs, PIASs, pET-E1/E2/SUMO1 and pET-E1/E2/SUMO2 were provided from Dr. CH Chung (Seoul National University, Seoul, Korea). The Fis1, Mff, MiD49 and MiD51 plasmids have previously described (50) and were generous gifts from Dr. MT Ryan (LaTrobe University, Melbourne, Australia). Construction of pFADD shRNAs was described previously (5). For the construction of FADD-3UTR shRNA, the 60-nucleotide fragments containing sequences of human FADD-3UTR (forward 5`-gatccccgcagagaggtggagaactgttcaagagacagttctccacctctctgcttttta-3`, reverse 5`-agcttaaaaagcagagaggtggagaactgtctcttgaacagttctccacctctctgcg gg-3`) were synthesized, annealed and cloned into *Bgl*II and *Hin*dIII sites of pSuper.neo mammalian expression vector (OligoEgine, Seattle, WA, USA). For site-directed mutagenesis, all FADD SUMOylation mutants were generated by a Quickchange Site-Directed Mutagenesis Kit (Stratagene) using synthetic oligonucleotides containing mutations in the corresponding

positions to generate lysine-to-arginine mutation. All mutants were verified by DNA sequencing analysis.

Cell death assay

Cells were exposed with various stimuli and stained with Propidium Iodide (PI; 1μg/ml), after which necrotic cell death was assessed by counting the number of PI-positive cells showing plasma membrane destruction and ruptured morphology (> 300 cells) under a fluorescence microscope (Olympus, Tokyo, Japan).

Assays for SUMOylation

HA-FADD and His-SUMOs (-1, -2) were overexpressed in HEK293T cells with or without Flag-tagged Ubc9 or SENPs, PIASs. After culturing for 24 h, cells were lysed in denaturing buffer containing 150 mM Tris-HCl (pH 8.0), 5% SDS and 30% glycerol. Cell lysates were diluted 10-fold with buffer A consisting of 20 mM Tris-HCl (pH 8.0), 150 mM NaCl, 0.2% Triton X-100, 1 mM PMSF, and 1 μg/ml each of aprotinin, leupeptin, pepstatin A and 20 mM NEM. Following sonication, insoluble material was removed by centrifugation for 30min at 15000 *g*. After incubating them with Ni^{2+}-NTA-agarose (Quigen) for 3 h at 4℃, the resins were collected and

washed with buffer A. Bound proteins were eluted in SDS-sampling buffer and resolved by SDS-PAGE. His-SUMO conjugated proteins were detected by immunoblot analysis. For assaying SUMOylation of endogenous FADD, HeLa cells were treated with or without A23187 and lysed as above. The diluted lysates were incubated with anti-FADD antibody (G-4) or pre-immune serum for over-night at 4°C and then with protein G-Sepharose (GE healthcare) for the next 2 h. The resins were collected, washed with buffer A and boiled. Supernatants were subjected to SDS-PAGE followed by immunoblot analysis. For *in vitro* SUMOylation assay, purified GB1-FADD (2 mg), SUMO2 (2 mg), SAE1/SAE2 (0.5 mg), and Ubc9 (1 mg) were incubated with an ATP (2mM) of 50mM Tris-HCl (pH 7.5), 5mM $MgCl_2$, 2mM ATP in a total volume of 20 μl. After incubating the mixtures for 2 h at 37°C, they were boiled and subjected to SDS-PAGE followed by immunoblot analysis. For E.coli SUMOylation, pTE1E2S1 or pTE1E2S2 and pET-FADD were transformed into BL21 (DE3) strain. A single colony was selected and transferred to LB broth containing 50 mg/ml of chloramphenicol and 100 mg/ml of ampicillin. Bacterial cultures were incubated at 37°C until reaching an OD_{600} = 1.0, and then treated with 1 mM IPTG to the culture for 5 h at 25°C. 1 ml of the bacterial culture was collected by centrifugation and the pellet was boiled in SDS-sample buffer

and subjected to immunoblot assay.

Immunostaining

HeLa cells grown on coverslips in 12-well plates were fixed in 4% paraformaldehyde for 5 min, permeabilized with 0.005% digitonin in PBS (Gibco, 70011-044) for 5 min, and blocked with 1% BSA for 2 h. After blocking, the fixed cells were incubated with antibodies at 1:100 to 1:250 dilution ratio, followed by incubation with Alexa Fluor secondary antibodies (Molecular probes, A11005, A11001, A11008 and A11012) stained with antibody and Hoechst 33258. Samples were visualized under a confocal fluorescence microscope (Carl Zeiss, LSM700, Carl-Zeiss-Promenade 10, 07745, Jena Germany).

Isolation of mitochondrial-enriched fraction

Cells were washed with cold PBS and were subjected to sonication twice at 30% amplitude for 10 s with an Ultrasonic Processor 130 W (Sonics and Materials, Newtown, CT USA) in Buffer A (250 mM sucrose, 20 mM HEPES-NaOH, pH 7.5, 2 mM EGTA, pH 7.2, 10 mM KCl, 1.5 mM $MgCl_2$ at 4°C). Unbroken cells and nuclei were removed by centrifugation at 1,000 g for 10 min at 4°C. The post-nuclear supernatant fraction was pelleted by

further centrifugation at 10,000 g for 15 min to obtain the mitochondria pellet. The pellets were washed with Buffer B (1 mM EDTA, 10 mM Tris, pH 7.4) and spun at 10,000 *g* again for 20 minutes at 4°C. The final pellets were suspended in lysis buffer containing 1% Triton X-100 and were mitochondrial-rich lysate fractions. The mitochondrial membrane protein TOM20 was used as a marker and loading control.

The model of middle cerebral artery occlusion (MCAO)

C57BL/6 mice (male, 12 weeks, 20-25 g) were anesthetized with a PBS: zoletil: rompun mixture (60%: 35%: 5%) during surgical preparation by intraperitoneal injection. The right common carotid artery was isolated and a size 6-0 microfilament with silicon rubbed-coated tip, diameter 0.21 mm (Doccol Corporation, CA, USA) was inserted into the right MCA and pushed gently through lumen. After 30 min, the mice were sacrificed or followed reperfusion for 2 hours by withdrawing the suture. Sham-operated mice underwent same procedure except the MCA blocking. During the surgery and following reperfusion, body temperature was maintained in the range of 37 ± 1 °C.

Measurement of MPTP opening

Inner mitochondrial membrane permeability was assessed by quenching of Calcein-AM fluorescence by cobalt. Briefly, cells were incubated with 1 μM Calcein-AM and 1 mM $CoCl_2$ for 10 min and then treated with 20 μM A23187 for 3 h. Cells were imaged by confocal microscopy.

Statistical analyses.

All statistical analyses were performed using a two-tailed Student's *t*-test or one-way ANOVA followed by a SigmaStat software.

References

Babic I, Cherry E, Fujita DJ. 2006. SUMO modification of Sam68 en hances its ability to repress cyclin D1 expression and inhibits its abili ty to induce apoptosis. *Oncogene* **25**: 4955-4964.

Besnault-Mascard L, Leprince C, Auffredou MT, Meunier B, Bourgead e MF, Camonis J, Lorenzo HK, Vazquez A. 2005. Caspase-8 sumoylat ion is associated with nuclear localization. *Oncogene* **24**: 3268-3273.

Bischof O, Schwamborn K, Martin N, Werner A, Sustmann C, Grossc hedl R, Dejean A. 2006. The E3 SUMO ligase PIASy is a regulator of cellular senescence and apoptosis. *Molecular cell* **22**: 783-794.

Blomster HA, Hietakangas V, Wu J, Kouvonen P, Hautaniemi S, Sisto nen L. 2009. Novel proteomics strategy brings insight into the prevale nce of SUMO-2 target sites. *Molecular & cellular proteomics : MCP* **8**: 1382-1390.

Blomster HA, Imanishi SY, Siimes J, Kastu J, Morrice NA, Eriksson JE, Sistonen L. 2010. In vivo identification of sumoylation sites by a signature tag and cysteine-targeted affinity purification. *The Journal o f biological chemistry* **285**: 19324-19329.

Bonfoco E, Krainc D, Ankarcrona M, Nicotera P, Lipton SA. 1995. A poptosis and necrosis: two distinct events induced, respectively, by mil d and intense insults with N-methyl-D-aspartate or nitric oxide/superox ide in cortical cell cultures. *Proceedings of the National Academy of Sciences of the United States of America* **92**: 7162-7166.

Breckenridge DG, Stojanovic M, Marcellus RC, Shore GC. 2003. Casp ase cleavage product of BAP31 induces mitochondrial fission through endoplasmic reticulum calcium signals, enhancing cytochrome c release to the cytosol. *The Journal of cell biology* **160**: 1115-1127.

Brenner C, Moulin M. 2012. Physiological roles of the permeability tr ansition pore. *Circulation research* **111**: 1237-1247.

Buschmann T, Fuchs SY, Lee CG, Pan ZQ, Ronai Z. 2000. SUMO-1

modification of Mdm2 prevents its self-ubiquitination and increases M dm2 ability to ubiquitinate p53. *Cell* **101**: 753-762.

Cereghetti GM, Stangherlin A, Martins de Brito O, Chang CR, Blacks tone C, Bernardi P, Scorrano L. 2008. Dephosphorylation by calcineuri n regulates translocation of Drp1 to mitochondria. *Proceedings of the National Academy of Sciences of the United States of America* **105**: 1 5803-15808.

Chan DC. 2006. Mitochondria: dynamic organelles in disease, aging, a nd development. *Cell* **125**: 1241-1252.

Chaudhary PM, Eby MT, Jasmin A, Kumar A, Liu L, Hood L. 2000. Activation of the NF-kappaB pathway by caspase 8 and its homolog s. *Oncogene* **19**: 4451-4460.

Chen X, Wu J, Lvovskaya S, Herndon E, Supnet C, Bezprozvanny I. 2011. Dantrolene is neuroprotective in Huntington's disease transgenic mouse model. *Molecular neurodegeneration* **6**: 81.

Chinnaiyan AM, O'Rourke K, Tewari M, Dixit VM. 1995. FADD, a n ovel death domain-containing protein, interacts with the death domain of Fas and initiates apoptosis. *Cell* **81**: 505-512.

Choi DW. 1995. Calcium: still center-stage in hypoxic-ischemic neuron al death. *Trends in neurosciences* **18**: 58-60.

Choi WS, Lee EH, Chung CW, Jung YK, Jin BK, Kim SU, Oh TH, Saido TC, Oh YJ. 2001. Cleavage of Bax is mediated by caspase-de pendent or -independent calpain activation in dopaminergic neuronal ce lls: protective role of Bcl-2. *Journal of neurochemistry* **77**: 1531-1541.

Elmore S. 2007. Apoptosis: a review of programmed cell death. *Toxic ologic pathology* **35**: 495-516.

Endo H, Kamada H, Nito C, Nishi T, Chan PH. 2006. Mitochondrial translocation of p53 mediates release of cytochrome c and hippocampa l CA1 neuronal death after transient global cerebral ischemia in rats. *The Journal of neuroscience : the official journal of the Society for N euroscience* **26**: 7974-7983.

Gareau JR, Lima CD. 2010. The SUMO pathway: emerging mechanis ms that shape specificity, conjugation and recognition. *Nature reviews Molecular cell biology* **11**: 861-871.

Gill G. 2004. SUMO and ubiquitin in the nucleus: different functions, similar mechanisms? *Genes & development* **18**: 2046-2059.

Golebiowski F, Matic I, Tatham MH, Cole C, Yin Y, Nakamura A, C ox J, Barton GJ, Mann M, Hay RT. 2009. System-wide changes to S UMO modifications in response to heat shock. *Science signaling* **2**: ra 24.

Guo X, Sesaki H, Qi X. 2014. Drp1 stabilizes p53 on the mitochondr ia to trigger necrosis under oxidative stress conditions in vitro and in vivo. *The Biochemical journal* **461**: 137-146.

Gustafsson AB, Gottlieb RA. 2008. Heart mitochondria: gates of life and death. *Cardiovascular research* **77**: 334-343.

Hamahata K, Adachi S, Matsubara H, Okada M, Imai T, Watanabe K, Toyokuni SY, Ueno M, Wakabayashi S, Katanosaka Y et al. 2005. Mitochondrial dysfunction is related to necrosis-like programmed cell death induced by A23187 in CEM cells. *European journal of pharma cology* **516**: 187-196.

Harada K, Toyooka S, Shivapurkar N, Maitra A, Reddy JL, Matta H, Miyajima K, Timmons CF, Tomlinson GE, Mastrangelo D et al. 200 2. Deregulation of caspase 8 and 10 expression in pediatric tumors an d cell lines. *Cancer research* **62**: 5897-5901.

Hay RT. 2005. SUMO: a history of modification. *Molecular cell* **18**: 1-12.

Hsiao HH, Meulmeester E, Frank BT, Melchior F, Urlaub H. 2009. " ChopNSpice," a mass spectrometric approach that allows identification of endogenous small ubiquitin-like modifier-conjugated peptides. *Molec ular & cellular proteomics : MCP* **8**: 2664-2675.

Huang TT, Wuerzberger-Davis SM, Wu ZH, Miyamoto S. 2003. Sequ ential modification of NEMO/IKKgamma by SUMO-1 and ubiquitin m

ediates NF-kappaB activation by genotoxic stress. *Cell* **115**: 565-576.

Iglewski M, Hill JA, Lavandero S, Rothermel BA. 2010. Mitochondria l fission and autophagy in the normal and diseased heart. *Current hyp ertension reports* **12**: 418-425.

Ishihara N, Nomura M, Jofuku A, Kato H, Suzuki SO, Masuda K, Ot era H, Nakanishi Y, Nonaka I, Goto Y et al. 2009. Mitochondrial fiss ion factor Drp1 is essential for embryonic development and synapse f ormation in mice. *Nature cell biology* **11**: 958-966.

Johnson ES. 2004. Protein modification by SUMO. *Annual review of biochemistry* **73**: 355-382.

Juo P, Kuo CJ, Yuan J, Blenis J. 1998. Essential requirement for casp ase-8/FLICE in the initiation of the Fas-induced apoptotic cascade. *Cu rrent biology : CB* **8**: 1001-1008.

Kawahara A, Ohsawa Y, Matsumura H, Uchiyama Y, Nagata S. 1998. Caspase-independent cell killing by Fas-associated protein with death domain. *The Journal of cell biology* **143**: 1353-1360.

Kim H, Lee HJ, Oh Y, Choi SG, Hong SH, Kim HJ, Lee SY, Choi J W, Su Hwang D, Kim KS et al. 2014. The DUSP26 phosphatase acti vator adenylate kinase 2 regulates FADD phosphorylation and cell gro wth. *Nature communications* **5**: 3351.

Kim H, Scimia MC, Wilkinson D, Trelles RD, Wood MR, Bowtell D, Dillin A, Mercola M, Ronai ZA. 2011. Fine-tuning of Drp1/Fis1 avai lability by AKAP121/Siah2 regulates mitochondrial adaptation to hypo xia. *Molecular cell* **44**: 532-544.

Kischkel FC, Hellbardt S, Behrmann I, Germer M, Pawlita M, Kram mer PH, Peter ME. 1995. Cytotoxicity-dependent APO-1 (Fas/CD95)-a ssociated proteins form a death-inducing signaling complex (DISC) wit h the receptor. *The EMBO journal* **14**: 5579-5588.

Knott AB, Perkins G, Schwarzenbacher R, Bossy-Wetzel E. 2008. Mit ochondrial fragmentation in neurodegeneration. *Nature reviews Neurosci ence* **9**: 505-518.

Kristian T, Siesjo BK. 1998. Calcium in ischemic cell death. *Stroke; a journal of cerebral circulation* **29**: 705-718.

Lamy L, Ngo VN, Emre NC, Shaffer AL, 3rd, Yang Y, Tian E, Nair V, Kruhlak MJ, Zingone A, Landgren O et al. 2013. Control of auto phagic cell death by caspase-10 in multiple myeloma. *Cancer cell* **23**: 435-449.

Lee EW, Kim JH, Ahn YH, Seo J, Ko A, Jeong M, Kim SJ, Ro JY, Park KM, Lee HW et al. 2012. Ubiquitination and degradation of th e FADD adaptor protein regulate death receptor-mediated apoptosis an d necroptosis. *Nature communications* **3**: 978.

Lee HJ, Pyo JO, Oh Y, Kim HJ, Hong SH, Jeon YJ, Kim H, Cho D H, Woo HN, Song S et al. 2007. AK2 activates a novel apoptotic pat hway through formation of a complex with FADD and caspase-10. *Na ture cell biology* **9**: 1303-1310.

Lee PS, Chang C, Liu D, Derynck R. 2003. Sumoylation of Smad4, t he common Smad mediator of transforming growth factor-beta family signaling. *The Journal of biological chemistry* **278**: 27853-27863.

Liu T, Roh SE, Woo JA, Ryu H, Kang DE. 2013. Cooperative role o f RanBP9 and P73 in mitochondria-mediated apoptosis. *Cell death & disease* **4**: e476.

Markus R, Reutens DC, Kazui S, Read S, Wright P, Pearce DC, Toch on-Danguy HJ, Sachinidis JI, Donnan GA. 2004. Hypoxic tissue in is chaemic stroke: persistence and clinical consequences of spontaneous s urvival. *Brain : a journal of neurology* **127**: 1427-1436.

Matsumura H, Shimizu Y, Ohsawa Y, Kawahara A, Uchiyama Y, Nag ata S. 2000. Necrotic death pathway in Fas receptor signaling. *The Jo urnal of cell biology* **151**: 1247-1256.

McBride HM, Neuspiel M, Wasiak S. 2006. Mitochondria: more than just a powerhouse. *Current biology : CB* **16**: R551-560.

Mears JA, Lackner LL, Fang S, Ingerman E, Nunnari J, Hinshaw JE. 2011. Conformational changes in Dnm1 support a contractile mechani

sm for mitochondrial fission. *Nature structural & molecular biology* **18**: 20-26.

Meinecke I, Cinski A, Baier A, Peters MA, Dankbar B, Wille A, Drynda A, Mendoza H, Gay RE, Hay RT et al. 2007. Modification of nuclear PML protein by SUMO-1 regulates Fas-induced apoptosis in rheumatoid arthritis synovial fibroblasts. *Proceedings of the National Academy of Sciences of the United States of America* **104**: 5073-5078.

Melchior F, Schergaut M, Pichler A. 2003. SUMO: ligases, isopeptidases and nuclear pores. *Trends in biochemical sciences* **28**: 612-618.

Miyauchi Y, Yogosawa S, Honda R, Nishida T, Yasuda H. 2002. Sumoylation of Mdm2 by protein inhibitor of activated STAT (PIAS) and RanBP2 enzymes. *The Journal of biological chemistry* **277**: 50131-50136.

Moujalled DM, Cook WD, Murphy JM, Vaux DL. 2014. Necroptosis induced by RIPK3 requires MLKL but not Drp1. *Cell death & disease* **5**: e1086.

Orabi AI, Shah AU, Ahmad MU, Choo-Wing R, Parness J, Jain D, Bhandari V, Husain SZ. 2010. Dantrolene mitigates caerulein-induced pancreatitis in vivo in mice. *American journal of physiology Gastrointestinal and liver physiology* **299**: G196-204.

Otera H, Ishihara N, Mihara K. 2013. New insights into the function and regulation of mitochondrial fission. *Biochimica et biophysica acta* **1833**: 1256-1268.

Park WS, Lee JH, Shin MS, Park JY, Kim HS, Lee JH, Kim YS, Lee SN, Xiao W, Park CH et al. 2002. Inactivating mutations of the caspase-10 gene in gastric cancer. *Oncogene* **21**: 2919-2925.

Pichler A, Knipscheer P, Oberhofer E, van Dijk WJ, Korner R, Olsen JV, Jentsch S, Melchior F, Sixma TK. 2005. SUMO modification of the ubiquitin-conjugating enzyme E2-25K. *Nature structural & molecular biology* **12**: 264-269.

Reed JC. 2002. Apoptosis-based therapies. *Nature reviews Drug discov*

ery **1**: 111-121.

Ren J, Gao X, Jin C, Zhu M, Wang X, Shaw A, Wen L, Yao X, Xue Y. 2009. Systematic study of protein sumoylation: Development of a site-specific predictor of SUMOsp 2.0. *Proteomics* **9**: 3409-3412.

Sheng B, Wang X, Su B, Lee HG, Casadesus G, Perry G, Zhu X. 2012. Impaired mitochondrial biogenesis contributes to mitochondrial dysfunction in Alzheimer's disease. *Journal of neurochemistry* **120**: 419-429.

Shin MS, Kim HS, Kang CS, Park WS, Kim SY, Lee SN, Lee JH, Park JY, Jang JJ, Kim CW et al. 2002. Inactivating mutations of CASP10 gene in non-Hodgkin lymphomas. *Blood* **99**: 4094-4099.

Shirendeb U, Reddy AP, Manczak M, Calkins MJ, Mao P, Tagle DA, Reddy PH. 2011. Abnormal mitochondrial dynamics, mitochondrial loss and mutant huntingtin oligomers in Huntington's disease: implications for selective neuronal damage. *Human molecular genetics* **20**: 1438-1455.

Smirnova E, Griparic L, Shurland DL, van der Bliek AM. 2001. Dynamin-related protein Drp1 is required for mitochondrial division in mammalian cells. *Molecular biology of the cell* **12**: 2245-2256.

Smith M, Mallin DR, Simon JA, Courey AJ. 2011. Small ubiquitin-like modifier (SUMO) conjugation impedes transcriptional silencing by the polycomb group repressor Sex Comb on Midleg. *The Journal of biological chemistry* **286**: 11391-11400.

Teitz T, Wei T, Valentine MB, Vanin EF, Grenet J, Valentine VA, Behm FG, Look AT, Lahti JM, Kidd VJ. 2000. Caspase 8 is deleted or silenced preferentially in childhood neuroblastomas with amplification of MYCN. *Nature medicine* **6**: 529-535.

Uchimura Y, Nakao M, Saitoh H. 2004. Generation of SUMO-1 modified proteins in E. coli: towards understanding the biochemistry/structural biology of the SUMO-1 pathway. *FEBS letters* **564**: 85-90.

Varadi A, Johnson-Cadwell LI, Cirulli V, Yoon Y, Allan VJ, Rutter G

A. 2004. Cytoplasmic dynein regulates the subcellular distribution of mitochondria by controlling the recruitment of the fission factor dyna min-related protein-1. *Journal of cell science* **117**: 4389-4400.

Wang J, Zheng L, Lobito A, Chan FK, Dale J, Sneller M, Yao X, P uck JM, Straus SE, Lenardo MJ. 1999. Inherited human Caspase 10 mutations underlie defective lymphocyte and dendritic cell apoptosis in autoimmune lymphoproliferative syndrome type II. *Cell* **98**: 47-58.

Wang Z, Jiang H, Chen S, Du F, Wang X. 2012. The mitochondrial phosphatase PGAM5 functions at the convergence point of multiple ne crotic death pathways. *Cell* **148**: 228-243.

Welz PS, Wullaert A, Vlantis K, Kondylis V, Fernandez-Majada V, Er molaeva M, Kirsch P, Sterner-Kock A, van Loo G, Pasparakis M. 201 1. FADD prevents RIP3-mediated epithelial cell necrosis and chronic i ntestinal inflammation. *Nature* **477**: 330-334.

Whelan RS, Konstantinidis K, Wei AC, Chen Y, Reyna DE, Jha S, Y ang Y, Calvert JW, Lindsten T, Thompson CB et al. 2012. Bax regula tes primary necrosis through mitochondrial dynamics. *Proceedings of t he National Academy of Sciences of the United States of America* **10 9**: 6566-6571.

Yu G, Zucchi R, Ronca-Testoni S, Ronca G. 2000. Protection of ische mic rat heart by dantrolene, an antagonist of the sarcoplasmic reticulu m calcium release channel. *Basic research in cardiology* **95**: 137-143.

Zhang H, Zhou X, McQuade T, Li J, Chan FK, Zhang J. 2011. Funct ional complementation between FADD and RIP1 in embryos and lymp hocytes. *Nature* **471**: 373-376.

Zhang J, Winoto A. 1996. A mouse Fas-associated protein with homol ogy to the human Mort1/FADD protein is essential for Fas-induced ap optosis. *Molecular and cellular biology* **16**: 2756-2763.

국문 초록

Fas-associated protein with death domain (FADD)은 외인성 세포사멸시에 개시 caspase 들을 끌어오고 활성화 시키는데 중요한 역할을 한다. 그러나 많은 증거들에 따르면 FADD 는 내인성 세포사멸, 세포증식, 외인성 세포괴사(necroptosis) 등의 다양한 신호 전달에도 관여되어 있다.

본인은 FADD 의 120 번/125 번/149 번째의 lysine 기에 SUMO2 (수모 2)의 결합이 유도됨을 밝혔다. 이 수모화는 E3 결합요소인 PIAS3 에 의해 매개되고, SENP6, 7 에 의해 수모기가 떨어진다. FADD 의 수모화는 세포괴사를 유도하는 높은 농도의 A23187 이 HeLa 세포에 처리 되었을 때 일어난다. 세포 내에 calcium 과부하가 일어나면 FADD 가 미토콘드리아로 이동하며, 이는 Drp1 의 미토콘드리아로의 이동을 촉진한다. A23187 처리에 의해 일어나는 Drp1 에 의한 미토콘드리아의 fragmentation 은 FADD 의 수모화에 의존적인 방식으로 일어난다. A23187 에 의해 일어나는 세포괴사는 Drp1 또는 FADD 가 없는 MEF 세포에서 또는 수모화에 결함이 있는 FADD 3KR 돌연변이가 발현되었을 경우에도 억제된다. Drp1 은 수모화된 FADD 와 in vitro 상에서

또는 세포 안에서 직접 결합을 한다. 결합한 FADD 와 Drp1 은 mitochondria 외막에 있는 수용체인 Mff 에 붙는다. 이런 FADD 의 수모화와 미토콘드리아로의 이동은 허혈성 환경에서 키운 세포 안에서 calcium 에 의존적으로 일어나며, middle cerebral artery 의 결찰을 통해 쥐의 뇌 안에 허혈성 손상을 일으켰을 때도 일어난다. 놀랍게도, calcium 의 과부하에 의한 세포 죽음은 caspase-10 의 발현 저하에 의해 억제되며 caspase-8 에 의해서는 저해되지 않는다. 그러나 A23187 그리고 미토콘드리아의 FADD 에 의한 미토콘드리아의 fragmentation 은 caspase 의 활성에 의존적이지 않은 괴사성 죽음을 일으킨다. 흥미롭게도, caspase-10 은 FADD 와 Drp1 의 complex 에 구성되며 A23187 에 의한 세포괴사와 Drp1 의 oligomerization 을 촉진한다. 특히, autoimmune lymphoproliferative syndrome 에서 보여지는 활성도가 없는 caspase-10 V410I 와 L285F 돌연변이는 TRAIL 에 의한 세포사멸을 억제하는 반면 Drp1 의 oligomerization 은 증가시킨다.

종합적으로, 이 연구는 calcium 과부하에 의한 Drp1 그리고 caspase-10 의존적인 미토콘드리아의 fragmentation 그리고

그에 따른 세포괴사를 유발하는 FADD 의 새로운 수모화 변형을 밝혔고, 다양한 병리 상황 중 허혈성 손상에서의 분자적 기전의 이해를 넓혔다.

Key words: FADD (Fas-associated protein with a death domain), Drp1 (Dynamin-related protein 1), mitochondrial fragmentation, caspase-10, PIAS3 (protein inhibitor of activated STAT3), regulated necrosis, SMOylaiton

Student Number : 2007-22808